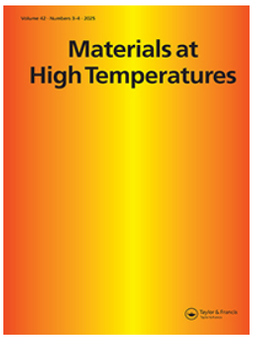

Materials at High Temperatures

ISSN: 0960-3409 (Print) 1878-6413 (Online) Journal homepage: www.tandfonline.com/journals/ymht20

The role of primary and tertiary creep in defining the form of the Monkman-Grant relation using the 4-θ methodology: an application to Waspaloy

Mark Evans

To cite this article: Mark Evans (05 Oct 2025): The role of primary and tertiary creep in defining the form of the Monkman-Grant relation using the 4-θ methodology: an application to Waspaloy, Materials at High Temperatures, DOI: 10.1080/09603409.2025.2556580

To link to this article: https://doi.org/10.1080/09603409.2025.2556580

Published online: 05 Oct 2025.

MATERIALS AT HIGH TEMPERATURES
https://doi.org/10.1080/09603409.2025.2556580

Taylor & Francis
Taylor & Francis Group

The role of primary and tertiary creep in defining the form of the Monkman-Grant relation using the 4-θ methodology: an application to Waspaloy

Mark Evans

Institute of Structural Materials, Swansea University Bay Campus, Swansea, UK

ABSTRACT

It is important to be able to predict the life of materials at high temperatures and an analysis of minimum creep rates vs. time to failure is one way of approaching this problem. However, recent studies on 9Cr steels, for example, have shown that this Monkman-Grant plot exhibits a low overall value for the exponent on the minimum creep rate ($\rho = -0.85$), together with a substantial scatter of data points around the relation. Both these phenomena, together with it being a mainly empirical relation, have restricted its use for life prediction purposes and so this paper aims to identify the causes of these two phenomena and to provide an explanation of this relation based on creep mechanisms. This is done within the 4-θ methodology so that the roles played by hardening, softening and damage mechanisms in causing this large scatter and low ρ value can be explicitly quantified. By manipulating the 4-θ equations, it was found that the role played by hardening and softening in identifying the form of the Monkman-Grant relation is restricted to the determination of a theoretical secondary creep rate measured as $\theta_3\theta_4$ - the exponent on which is predicted to equal −1 in this methodology. However, the data obtained on Waspaloy revealed ρ to equal −0.778 over all test conditions. This paper demonstrated that this was caused by the Monkman-Grant proportionality constant falling into three well defined groupings depending on values for both the amount of accumulated damage and the rate at which this damage occurred in a test specimen. It then turned out that within each such grouping, the exponent on the secondary creep rate equalled −1 as suggested by the 4-θ methodology. Then, by considering the damage at failure and the rate of its accumulation in the determination of the Monkman-Grant proportionality constant, together with the replacement of the minimum creep rate with $\theta_3\theta_4$, resulted in a Monkman-Grant exponent of −1 with minimal scatter around this relation.

ARTICLE HISTORY
Received 10 June 2025
Accepted 31 August 2025

KEYWORDS
Waspaloy; Monkman-Grant relation; 4-θ methodology; damage; rates of damage accumulation; recovery; hardening

Introduction

Waspaloy is a nickel-based superalloy used primarily in high-temperature and high-stress applications, especially in the aerospace and power generation industries. It has excellent creep and oxidation resistance at elevated temperatures, especially up to temperatures of around 1140K. The main aerospace components made with this material include turbine discs, compressor wheels, blades, seals, shafts and spacers. In gas turbine engines, Waspaloy is used in the manufacture of combustion chambers, afterburner components and turbine section components. A gas turbine disc typically operates in the range 923K to 1023K, compressor rotors at temperatures between 673K to 923K and combustor ducts at temperatures between 1023K to 1140K. Compressor blades used in the high-pressure section of the engine, typically experience a centrifugal stress of between 300 and 600 MPa and a bending stress between 50 and 150 MPa. High-pressure compressor discs typically experience a centrifugal hoop stress of between 500 and 900 MPa and an axial stress from blade loading of between 100 and 300 MPa. For the safe and economic operation of turbine blades, a creep rupture life in the time range of 20,000 to 25,000 hours for commercial engines is required (but 10,000–15,000 hours for military or high-performance engines) and for turbine discs a creep rupture life in the time range of 30,000 to 50,000 hours is required.

Evaluation of such longer-term creep rupture is typically done using accelerated creep tests (either accelerated stresses and/or temperatures), with creep models then being used to extrapolate to the lower stresses observed in the above-mentioned systems. However, there is little agreement on what creep models extrapolate best with respect to stress and temperature, and whilst some more recently developed models have been shown to perform well at such extrapolation over a wide range of materials, they currently lack the theoretical backing that provides the additional confidence required for widespread adoption (for example, Yang et al. [1] and Wilshire et al. [2–6]). An analysis of minimum creep rates vs. time to failure – the so-called Monkman – Grant relation [7] – using accelerated test data is another suggested way to

CONTACT Mark Evans m.evans@swansea.ac.uk Institute of Structural Materials, Swansea University Bay Campus, Crymlyn Burrows, Swansea SA1 8EN, Wales, UK

evaluate long-term creep rupture by extrapolating this accelerated relation using lower minimum creep rates – because once the minimum rate of creep in an ongoing creep test at non accelerated stresses is obtained at an early stage of creep, its rupture life is readily evaluated from this accelerated relation without a need to extrapolate with respect to stress and/or temperature. But again, there is limited theoretical backing for this relation.

A relationship between time to failure t_F and the minimum creep rate $\dot{\varepsilon}_M$ was first put forward by Monkman and Grant [7] and is now commonly referred to as the Monkman – Grant relation (or MG for short). They studied several materials (including, but not exclusively, Aluminium, Titanium 75, Ferritic Steels, Austenitic Steels and Inco 700) and identified the following relation

$$t_F = \frac{M}{(\dot{\varepsilon}_M)^{\rho}} \tag{1a}$$

where these authors found that the parameters ρ and M were constant over all the test conditions contained within the data sets that they analysed, but that they differed in value from material to material. (M is frequently termed the Monkman-Grant proportionality constant and ρ the Monkman-Grant exponent). For the materials investigated by these authors, ρ was close to 1 but varied between a low of 0.77 and a high of 0.93 (for Austenitic Steels). Likewise, M varied from a low of 0.48 to a high of 1.3 (for Aluminium). In the same year, and independently of Monkam and Grant, Machlin [8] provided a theoretical explanation of Eq (1a).

At a specific test condition, and when ρ = 1, the Monkman-Grant equation is a simple tautology or identity (represented by the symbol ≡). To see this, consider Figure 1, showing a hypothetical creep curve containing primary, secondary and tertiary creep obtained at a fixed stress and temperature. The observed minimum creep rate $\dot{\varepsilon}_M$ is equal to the gradient of the creep curve at the point of inflection, and the dashed line has such a slope – but has been extrapolated to time zero and to the time at failure. By the definition of a gradient, the slope of this line equals the vertical distance M divided by the time to failure t_F

$$\dot{\varepsilon}_M \equiv \frac{M}{t_F} \tag{1b}$$

and so, upon rearranging

$$t_F \equiv \frac{M}{\dot{\varepsilon}_M} \equiv M(\dot{\varepsilon}_M)^{-1} \tag{1c}$$

From this perspective, the Monkman-Grant relation requires the additional assumption that M is the same at all stresses and temperatures (subject to stochastic or random experimental variation). This assumption then turns this simple identity into a useful model or casual relation, because it then follows that a fall in $\dot{\varepsilon}_M$ must led to an increase in the time to failure (rather than to a change in M).

Since this relation was first identified, some doubt has been cast as to the constancy of M and ρ with respect to test conditions. For example, when studying 9Cr-1Mo steel, Abe [9] and Choudary [10] have shown M and ρ are different in value at long failure times (i.e. at lower stresses) compared to short and intermediate failure times. More specifically, they found that over most test conditions ρ = 1, but at the lower stresses leading to the longest failure times, ρ fell below 1. In order to explain the change in values for M

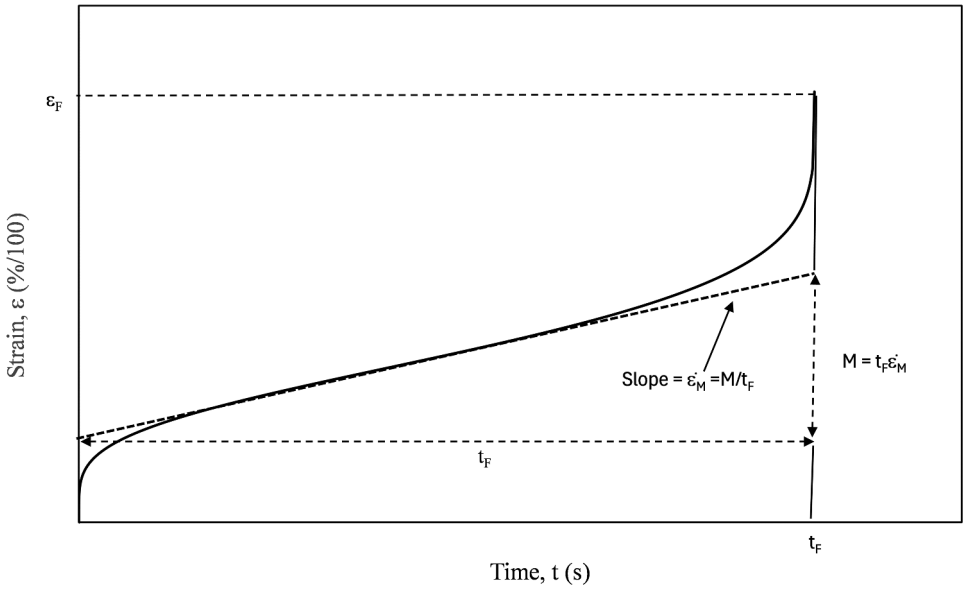

Figure 1. Schematic representation of a uniaxial creep curve obtained at a constant stress and temperature.

and ρ at lower stresses, several modifications of Eq (1a) have been proposed. Dobes and Milicka [11] proposed the following modified form

$$\frac{t_F}{\varepsilon_F} = \frac{M_1}{(\dot{\varepsilon}_M)^{\rho_1}} \text{ with } \rho_1 = 1 \tag{1d}$$

where ε_F is the strain at failure. Subsequent authors have found some success with this modification. For example, Sklenicka et al. [12] studied a Gr. 92 steel and found a stable value for ρ_1 of 0.96 in Eq (1d) – in contrast to ρ = 0.88 in Eq (1a). The MG relation in Eq (1d) is related to the creep damage tolerance parameter λ. This parameter measures the ability of a material to withstand local concentrations of strain accumulation without cracking,

$$\lambda = \frac{(\varepsilon_F - \varepsilon_p)}{t_F \dot{\varepsilon}_M} \cong \frac{\varepsilon_F}{t_F \dot{\varepsilon}_M} \cong \frac{1}{M_1} \tag{1e}$$

where ε_p is the strain reached at the end of primary creep. The approximation in Eq (1e) corresponds to test conditions where the magnitude and duration of primary creep is small in relation to failure time – so $\varepsilon_p \cong 0$. This approximation results in the MG proportionality constant in Eq (1d) being equal to the reciprocal of the damage tolerance parameter, $\lambda^{-1} \cong M_1$. λ values in the range 5–10 are though to ensure that the strain concentrations typically encountered during in service operation will not lead to premature cracking and failure.

Abe [9] attributed the deviation from the simple MG relation with ρ = 1 in long-term creep, to increases in dln(ε̇)/dε, and proposed the following MG relation

$$\frac{d\ln(\dot{\varepsilon})}{d\varepsilon} t_F = \left(\frac{t_F}{(t_F - t_M)}\right)(\dot{\varepsilon}_M)^{-1} \tag{1f}$$

where t_M is the time taken to reach the minimum creep rate, ε is the creep strain and ε̇ is the creep strain rate. However, when applied to 9Cr steel, Abe obtained a value for ρ that was still less than 1.

Maruyama et al. [13] studied this phenomenon of ρ < 1 in more detail, using data on 9Cr-1Mo (Grade 92) steel. They found that the value for ρ differed over four different regions of stress and temperature, where each of these regions corresponded to different creep mechanisms. Whilst the value for ρ over all tests was 0.85, they found it to be especially low (0.62) in a region corresponding to values of stress and temperature that induced long times to failure (in excess of 10^4 hours). With long-term data points deviating from an MG relation determined by short-term data points, it becomes impossible to use this relationship to evaluate long-term life from short-term data.

These authors then went onto to study the role played by creep curve shape in determining the values for M and ρ using the following equation

$$\varepsilon = A\ln(1 + \alpha\ t) - B\ln(1 - \beta\ t) \tag{2a}$$

where t is the time and where A and B are parameters related to strain, whilst α and β are rate parameters. A (approximately) measures the decelerating rate of creep during primary creep (A = −1/(dln ε̇/dε)), and B measures creep rate acceleration (B = 1/(dln ε̇/dε)) in tertiary creep. Hence, A and B can be taken as summary measures of creep curve shape. They found that the values of A and B decreased with increasing creep rupture life, and it was this changing shape with t_F that explained the ρ values of less than unity, i.e. ρ is lowest when A and B are lowest. From this analysis, they found that constraining M to a value of

$$M = \left(\sqrt{A} + \sqrt{B}\right)^2 \tag{2b}$$

in Eq (1a) resulted in the Monkman-Grant exponent of ρ = 1 when applied to all the data on Grade 92 steel (both long and short-term tests results).

Abe [14] recently found that the following modified Monkman-Grant relation was in complete agreement with this work by Maruyama et al.

$$\frac{t_F}{\varepsilon_P} = C(\dot{\varepsilon}_M)^{-1} \tag{2c}$$

The better fit to the data obtained using this expression reflected the observation by the author that for 9Cr steel data ε_P was inversely proportional to $\dot{\varepsilon}_M$ over a wide range of test conditions and test durations.

However, Eq (2a) is purely empirical in nature and its parameters have not been explained in terms of creep mechanisms. The aim of this paper is therefore to identify a modified Monkman-Grant relation whose parameters can be explained in terms of creep processes such as hardening, softening and damage mechanisms. It is hope that providing such a theoretical basis will encourage the use of the relation for creep life prediction. To do this, a similar material to that studied by Maruyama et al. [13] was selected – namely a Grade 12 steel – but the creep equation used was that from the 4-θ methodology developed by Evans and Wilshire [15]

$$\varepsilon = \theta_1\left(1 - e^{-\theta_2 t}\right) + \theta_3\left(e^{\theta_4 t} - 1\right) \tag{2d}$$

where θ_1 are the four theta parameters that relate strain to time. θ_2 and θ_4 are rate parameters and θ_1 and θ_3 scale parameters – so, and for example, the strain obtained by the end of primary creep is given by θ_1. The reason for selecting this methodology is that the form of this equation has already been derived from an analysis of mechanisms governing creep [16]. Eqs (2a, 2c) are quite similar in nature with the main differences being seen in terms of creep rates: θ_2 = -ln(d ε̇/dε) and θ_4 = ln(d ε̇/dε).

The use of the 4-θ methodology enables deviations from the Monkman-Grant relation of Eq (1b) to be

explained not just in terms of creep curve shape, but also mechanisms of creep. More specifically, this paper will derive a MG relation from the 4-θ methodology to gain insights into the roles played by creep hardening, softening and damage mechanisms in determining the form of the MG relation – and indeed whether these mechanisms change with test conditions. This will then enable insights to be made as to whether and how the MG relation in short-term data can be used to evaluate long-term rupture. To achieve these aims, the paper is structured as follows. The next section describes the creep tests carried out on Waspaloy, and this is followed by a method section outlining how an MG relation can be derived from the 4-θ methodology. This modified relation is then applied to data on 12Cr steel in the results section. Finally, the conclusion section outlines areas for future work.

The data

This section describes the used in this paper in more detail. Thirty-one cylindrical test pieces were machined from a as received Waspaloy bar, with a gauge length of 28 mm and a diameter of 5 mm. The chemical composition of this batch of material is shown in Table 1. The material was heat treated for 4 h at 1353 K (water quenched), 4 h at 1123 K (air cooled) and 16 h at 1033 K (air cooled). This resulted in a uniform equiaxed structure of average grain diameter 45 μm. The microstructure contained uniform γ' particles of mean diameter 0.3 μm.

The tensile strength (σ_{TS}) values for this batch of material are shown in Table 2.

The specimens were tested in tension over a range of stresses at 873K, 923K, 973K and 1023K using high precision Andrade-Chalmers constant-stress machines. Loads and stresses could be applied and maintained to an accuracy of 0.5%. Up to 403 creep strain/time readings were taken during each of these tests. In all cases, temperatures were controlled along the gauge lengths and with respect to time to better than ± 1 K. The extensometer could measure tensile strain to better than 10^{-5}. Loading machines, extensometers and thermocouples were all calibrated with respect to NPL traceable standards. At 873K, eight specimens were placed on test over the stress range 1150 MPa to 700 MPa, at 923K seven specimens were placed on test over the stress range 1000 MPa to 550 MPa, at 973K nine specimens were placed on test over the stress range 950 MPa to 200 MPa and at 1023K seven specimens were tested over the stress range 700 MPa to 250 MPa. Figure 2 shows the normalised creep curves obtained at 923K. Because Waspaloy can serve at temperatures up to 920K for critical applications and 1040K for less demanding situations, the test programme covered stress ranges giving creep lives up to 5,500 h (around 19,852,000 s) at 873–1023 K. This data set has been published by Evans [16] and Wilshire and Scharning [17].

Methodology

Overview of the 4-θ methodology

The theta methodology given by Eq (2d) started out as a purely empirical equation to represent the shape of a uniaxial creep curve obtained at constant stress and temperature. As such it attracted the criticism that it lacked theoretical foundations and could not be related to the mechanisms of creep. Some 20 years later, one of the founders of the methodology rectified this position by explaining the form of Eq (2d) in terms of different hardening, softening and damage mechanism. In particular, Evans [16] showed that

$$\varepsilon = \frac{1}{\hat{H}\dot{\varepsilon}_o}\left[\dot{\varepsilon}_o - \frac{\hat{R}}{\hat{H}}\right]\left(1 - e^{-\hat{H}\dot{\varepsilon}_o t}\right) + \frac{1}{\hat{W}}\left(e^{\frac{\hat{W}\hat{R}}{\hat{H}}t} - 1\right)$$

where $\dot{\varepsilon}_o$ is the initial rate of creep and $\hat{H}$, $\hat{R}$ and $\hat{W}$ are constants determining the rate of hardening, softening and damage accumulation as a function of the rate of strain (to be defined more precisely in the following sub section). In comparison to Eq (2d) it follows that these important rate constants can be quantified from the four theta parameters as

$$\dot{\varepsilon}_o = \theta_1\theta_2 + \theta_3\theta_4; \hat{H} = \frac{\theta_2}{\dot{\varepsilon}_o}; \hat{R} = \frac{\theta_2\theta_3\theta_4}{\dot{\varepsilon}_o}; \hat{W} = \frac{1}{\theta_3}$$

The importance of all of this to an understanding of the Monkman-Grant relation has, however, not been examined. The contribution of this paper to this existing knowledge is therefore to show that this model of creep implies a Monkman-Grant relation of the form

Table 1. Chemical composition of Waspaloy weight %).

Cr	Co	C	Mn	Si	Fe	Mo	Ti	Al	B	Zr	S	P	Cu
19.1	13.5	0.03	0.1	0.1	0.79	4.08	3.15	1.3	0.005	0.07	0.0025	0.01	0.1

Also 5 ppm of Ag, 10 ppm of Pb and 0.5 ppm of Bi with balance Ni.

Table 2. Variation of tensile strength with temperature.

Temperature (K)	873	923	973	1023
Tensile Strength (MPa)	1154	1120	975	827

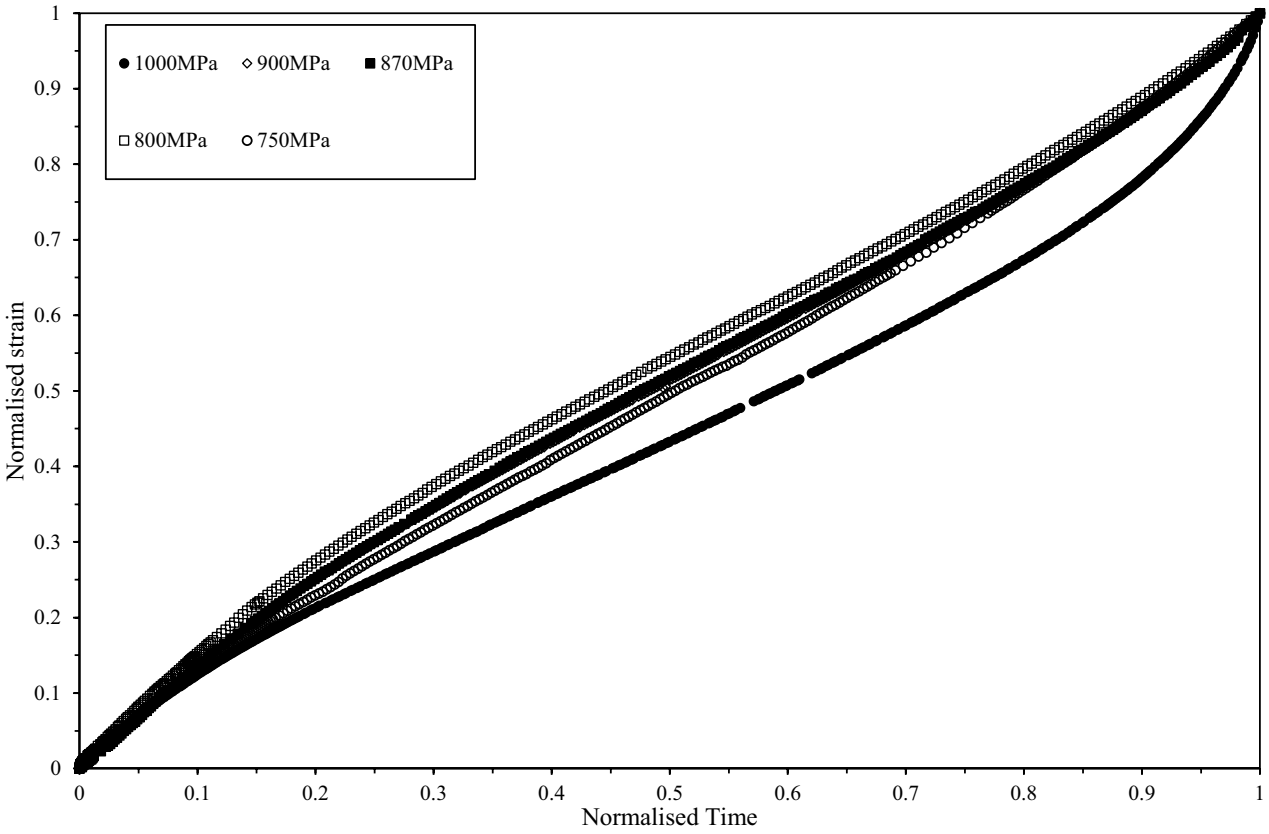

Figure 2. Normalised uniaxial creep curves obtained at various stresses at 923K.

$$t_F \approx \frac{1}{\hat{W}}\ln[1+W_F]\left(\dot{\varepsilon}_S\right)^{-1} = M_2\left(\dot{\varepsilon}_S\right)^{-1}$$

where $\dot{\varepsilon}_s = \frac{\hat{R}}{\hat{H}}$ is the theoretical secondary creep rate determined by the relative rates of hardening and softening and W_F is the amount of damage accumulated by the time of failure. Thus, this paper reveals in more detail below that the Monkman-Grant constant is a positive function of damage at failure and a negative function of the rate of damage accumulation. In this paper, these findings are tested on data collected on Waspaloy.

Creep mechanisms behind the 4-θ methodology

Based on Eq (2d), a specimen on test under uniaxial constant stress and temperature will eventually rupture with a failure time t_F and with a strain at rupture of ε_F

$$\varepsilon_F = \theta_1\left(1-e^{-\theta_2 t_F}\right)+\theta_3\left(e^{\theta_4 t_F}-1\right) \tag{3a}$$

Given that $-\theta_2$ is a small negative number and t_F a large number, $e^{-\theta_2 t_F} \approx 0$ and so

$$\varepsilon_F \approx \theta_1+\theta_3\left(e^{\theta_4 t_F}-1\right) \tag{3b}$$

which can be re-arranged for the time to failure

$$\begin{aligned} t_F &\cong \frac{1}{\theta_4}\ln\left[\frac{\varepsilon_F-\theta_1+\theta_3}{\theta_3}\right] = \frac{1}{\theta_4}\ln\left[1+\frac{\varepsilon_F-\theta_1}{\theta_3}\right] \\ &\cong \frac{1}{\theta_4}\ln\left[1+\frac{\varepsilon_F-\varepsilon_p}{\theta_3}\right] \end{aligned} \tag{3c}$$

where $\theta_p=\theta_1$. Although not obvious, Eq (3c) is a variant of the Monkman-Grant relation. To see this requires an understanding of the creep mechanisms behind Eq (2d) and this was first outlined by Evans [16]. Following this approach, internal state variables can be used to explain the form of Eq (3a) using as a starting point the following creep constitutive law for the strain rate $\underline{\dot{\varepsilon}}$

$$\dot{\varepsilon} = \Phi\left(\sigma, T, \xi_1, \xi_2, \ldots, \xi_\alpha, \ldots, \xi_p\right) \tag{4a}$$

where σ is stress, T absolute temperature, ξ_α are the internal state variables which are time dependent and $\Phi()$ is (an unknown) functional form. Each of these internal variables will have an equation associated with them that describes their evolution through time. All the ξ_α describe continuum quantities that could be classified as either hardening or softening, static or dynamic, transitory or permanent. One possible functional form for Eq (4a) is

$$\dot{\varepsilon} = \dot{\varepsilon}_o f(\xi_\alpha) \tag{4b}$$

where $\dot{\varepsilon}_o$ is the initial rate of strain occurring for virgin material when placed on test – and this will depend on

both stress and temperature. Here, $f(\xi_\alpha)$ takes on the value one for such material but thereafter is modified by the creep processes occurring within the grains and/or grain boundaries. Next, Evans assumed that $f(\xi_\alpha)$ is a linear function of these internal variables

$$\dot{\varepsilon} = \dot{\varepsilon}_o\{1 + (h_1 + .. + h_\alpha + .. + h_{mh}) + (r_1 + .. + r_\alpha + .. + r_{mr}) + (w_1 + .. + w_\alpha + .. + w_{mw})\} \quad (4c)$$

where h_α, r_α, and w_α are hardening, softening and damage internal variables respectively.

Softening (or recovery) variables are static but positive variables. In Waspaloy, each of the r_α variables could include (but not exclusively so) the following mechanisms that are temperature sensitive [18–20]:

(i) The coarsening of the fine γ′ precipitates referred to as Ostwald ripening, especially at temperatures above approximately 1023K. This process involves the dissolution of smaller precipitates and the growth of larger ones, leading to a decrease in the number and density of the γ′ particles. As a result, the material's resistance to dislocation motion diminishes.
(ii) At higher temperatures (above 1223K), dynamic recrystallisation becomes the dominant softening mechanism. This process involves the formation of new, strain-free grains that replace deformed ones, leading to a reduction in dislocation density and an increase in grain size.
(iii) At intermediate temperatures, dislocation recovery processes such as climb and cross-slip can occur, leading to a reduction in dislocation density. This recovery softens the material by reducing the obstacles to dislocation movement.

On the other hand, hardening variables are dynamic in nature and will be negative in quantity. In Waspaloy, each of the h_α variables could include (but not exclusively so) the following mechanisms [21,22]:

(i) The precipitation of γ′ (Ni_3Al and Ni_3Ti) phase particles. These fine, coherent precipitates impede dislocation movement, enhancing the alloy's strength, particularly at elevated temperatures. The ageing process promotes the formation of these precipitates, contributing significantly to the alloy's high-temperature performance. This is the primary strengthening mechanism in Waspaloy.
(ii) Alloying elements such as molybdenum, cobalt, chromium, and titanium are dissolved in the nickel matrix, creating lattice distortions. These distortions hinder dislocation motion, thereby increasing the yield strength of the material. This mechanism is particularly effective at higher temperatures, where the solid solution strengthening continues to play a significant role.
(iii) Elements like titanium and carbon form carbide precipitates (e.g. TiC) within the matrix and at grain boundaries. These carbides act as obstacles to dislocation movement and pin grain boundaries, preventing grain growth during high-temperature exposure.
(iv) At stresses above the yield point, dislocations multiply and interact, forming dislocation tangles or forests. These dense dislocation structures impede further dislocation movement, leading to increased strength through a mechanism known as forest hardening. This mechanism is particularly relevant during high-stress applications, such as turbine engine components.

The damage variables are usually dynamic in nature and positive in quantity. In Waspaloy, each of the w_α variables could include (but not exclusively so) the following mechanisms [23–25]:

(i) At elevated temperatures and stresses, Waspaloy undergoes grain boundary sliding, leading to the nucleation and growth of cavities at grain boundary triple points. These cavities can coalesce, forming micro voids that eventually lead to fracture. This process is particularly pronounced at temperatures between 973K and 1073K.
(ii) At high temperatures, the γ′ phase precipitates can dissolve or coarsen, reducing their effectiveness in impeding dislocation movement.
(iii) Carbides such as M_6C and M_6C_6 can precipitate at grain boundaries during service at elevated temperatures. While these carbides can strengthen the material, excessive precipitation can embrittle the grain boundaries, making them more susceptible to cracking under stress.
(iv) At stresses above the yield strength, dislocations accumulate and interact, forming dislocation tangles or forests. These structures impede further dislocation movement, leading to increased strength through forest hardening. However, at high temperatures, the mobility of dislocations increases, and the effectiveness of forest hardening diminishes.
(v) As Waspaloy is subjected to high temperatures and stresses, microstructural instabilities such as the coarsening of γ′ precipitates and the precipitation of carbides at grain boundaries can occur. These changes can lead to intergranular fracture, where cracks propagate along

the weakened grain boundaries, compromising the material's structural integrity

All these processes can be dependent or independent of each other, and the importance of a given process can vary with stress and temperature. Also, more than one process can occur at a time. Each mechanism will be a function of stress and temperature, but since these functional dependences may be different, the processes will contribute varying amounts to the creep process as conditions change. As the internal variables in Eq (4c) occur linearly, and because Eq (4c) is linear in the coefficients, it is possible to quantify the over-all hardening (H), softening (R) and damage (W) through a simple summation

$$H = \sum_{\alpha=1}^{mh} h_\alpha; R = \sum_{\alpha=1}^{mr} r_\alpha \text{ and } W = \sum_{\alpha=1}^{mw} w_\alpha \tag{4d}$$

Evans then postulated the following evolutionary equations for these internal variables

$$\dot{H} = -\hat{H}\dot{\varepsilon}; \dot{R} = \hat{R} \text{ and } \dot{W} = \hat{W}\dot{\varepsilon} \tag{4e}$$

where the dot above each variable refers to the rate of change in this variable with respect to time and $\hat{H}$, $\hat{R}$ and $\hat{W}$ are parameter constants found as

$$\hat{H} = \sum_{\alpha=1}^{mh} \hat{h}_\alpha; \hat{R} = \sum_{\alpha=1}^{mr} \hat{r}_\alpha \text{ and } \hat{W} = \sum_{\alpha=1}^{mw} \hat{w}_\alpha \tag{4f}$$

where $\dot{h}_\alpha = -\hat{h}_\alpha\dot{\varepsilon}$, $\dot{w}_\alpha = \hat{w}_\alpha\dot{\varepsilon}$ and $\dot{r}_\alpha = \hat{r}_\alpha$. Eq (4b) can then be written as

$$\dot{\varepsilon} = \dot{\varepsilon}_o(1 + H + R + W) \tag{4g}$$

At constant stress and temperature, $\hat{H}, \hat{R}$, and $\hat{W}$ are also constant, and if H = R = W = 0, when $t = 0$, then the differential of Eq (4g) with respect to time is

$$\ddot{\varepsilon} = \dot{\varepsilon}_o\left(\dot{H} + \dot{R}\right) = \dot{\varepsilon}_o\left(\hat{R} - \hat{H}\dot{\varepsilon}\right) \tag{5a}$$

for small times in relation to creep life, i.e. where the effects of W are negligible. Upon carrying out the following integration, which assumes damage over short periods of primary creep is negligible,

$$\int_{\dot{\varepsilon}_o}^{\dot{\varepsilon}} \frac{1}{\left(\hat{R} - \hat{H}\right)} d\dot{\varepsilon} = \dot{\varepsilon}_o \int_0^t dt$$

we get

$$\ln\left[\left(\hat{R} - \hat{H}\dot{\varepsilon}\right)\right] + C = -\hat{H}\dot{\varepsilon}_o t$$

where C is the constant of integration. When $t = 0$, $\dot{\varepsilon} = \dot{\varepsilon}_o$and so C = -ln($\left(\hat{R} - \hat{H}\dot{\varepsilon}_o\right)$. Thus

$$\ln\left[\frac{\left(\hat{R} - \hat{H}\dot{\varepsilon}\right)}{\left(\hat{R} - \hat{H}\dot{\varepsilon}_o\right)}\right] = -\hat{H}\dot{\varepsilon}_o t \tag{5b}$$

which upon re-arrangement and simplification yields

$$\dot{\varepsilon} = \left[\dot{\varepsilon}_o - \frac{\hat{R}}{\hat{H}}\right] e^{-\hat{H}\dot{\varepsilon}_o t} + \frac{\hat{R}}{\hat{H}} \tag{6a}$$

Eq (6a) states that an initial high creep rate of $\dot{\varepsilon}_o$, gives way to a rapidly decreasing creep rate until a steady state rate of creep equal to $\frac{\hat{R}}{\hat{H}}$ is reached. This can be interpreted as the theoretical secondary creep rate – that rate that would be observed if creep continued to progress without meaningful damage accumulation. Call this rate $\dot{\varepsilon}_S$ and so

$$\dot{\varepsilon}_S = \frac{\hat{R}}{\hat{H}} \tag{6b}$$

The value for this secondary creep rate is determined by the rate of work hardening $\hat{H}$ in relation to the rate of softening $\hat{R}$ occurring during primary creep. This is a very general specification of creep to which a variety of different creep mechanisms can be attached.

The Monkman-Grant relation and damage

Another key assumption behind Eq (2d), that is also key to a more in-depth understanding of the Monkman-Grant relation, is that damage W leads to strain rate accumulation by accelerating the secondary creep rate $\dot{\varepsilon}_S$

$$\dot{\varepsilon} = \left[\dot{\varepsilon}_o - \frac{\hat{R}}{\hat{H}}\right] e^{-\hat{H}\dot{\varepsilon}_o t} + \frac{\hat{R}}{\hat{H}}[1 + W] \tag{7a}$$

or, upon extracting all primary creep

$$\dot{\varepsilon}_T = \frac{\hat{R}}{\hat{H}}[1 + W] \tag{7b}$$

where $\dot{\varepsilon}_T$ is the tertiary strain rate. This can be rewritten in terms of time t by first noting that

$$\ddot{\varepsilon}_T = \frac{\hat{R}}{\hat{H}}\ [\dot{W}] = \frac{\hat{R}}{\hat{H}}\hat{W}\dot{\varepsilon}_T$$

so that

$$\int \frac{1}{\hat{W}\dot{\varepsilon}_T} d\dot{\varepsilon}_T = \frac{\hat{R}}{\hat{H}} \int dt$$

Thus

$$\frac{1}{\hat{W}}\ln[\dot{\varepsilon}_T] = \frac{\hat{R}}{\hat{H}}t + \mathrm{C}$$

with C $\cong \frac{1}{\hat{W}}\ln\left[\frac{\hat{R}}{\hat{H}}\right]$ and so upon further simplification

$$\dot{\varepsilon}_T = \frac{\hat{R}}{\hat{H}} e^{\frac{\hat{R}}{\hat{H}}\hat{W}t} \tag{7c}$$

Substituting this into Eqs (7a,7b)gives

$$\dot{\varepsilon} = \left[\dot{\varepsilon}_o - \frac{\hat{R}}{\hat{H}}\right] e^{-\hat{H}\dot{\varepsilon}_o t} + \frac{\hat{R}}{\hat{H}} e^{\frac{\hat{W}\hat{R}}{\hat{H}}t} \tag{8a}$$

and upon integration

$$\varepsilon = \frac{1}{\hat{H}\dot{\varepsilon}_o}\left[\dot{\varepsilon}_o - \frac{\hat{R}}{\hat{H}}\right]\left(1 - e^{-\hat{H}\dot{\varepsilon}_o t}\right) + \frac{1}{\hat{W}}\left(e^{\frac{\hat{W}\hat{R}}{\hat{H}}t} - 1\right) \tag{8b}$$

A comparison of Eq (8b) with Eq (2d) reveals that $\theta_4 = \hat{W}\frac{\hat{R}}{\hat{H}} = \hat{W}\,\dot{\varepsilon}_s$ and $\theta_3 = 1/\hat{W}$. Using this measure of the minimum creep rate allows Eq (3c) to be written as

$$t_F \approx \frac{1}{\theta_4}\ln\left[1 + \frac{\varepsilon_F - \varepsilon_p}{\theta_3}\right] = \theta_3 \ln\left[1 + \frac{\varepsilon_F - \varepsilon_p}{\theta_3}\right](\dot{\varepsilon}_S)^{-1} \tag{9a}$$

This is a Monkman-Grant type relation with $M_2 = \theta_3 \ln\left[1 + \frac{\varepsilon_F - \varepsilon_p}{\theta_3}\right]$. To further interpret the meaning of M_2, it can be noted that the amount of damage accumulated by the time of failure W_F can be calculated from Eqs (7b,7c)

$$1 + W_F = e^{\frac{\hat{R}}{\hat{H}}\hat{W}t_F}$$

But

$$e^{\frac{\hat{R}}{\hat{H}}\hat{W}t_F} = 1 + \hat{W}(\varepsilon_F - \varepsilon_p) \tag{9b}$$

and so

$$W_F = \hat{W}(\varepsilon_F - \varepsilon_p) \tag{9c}$$

This then allows Eq (9a) to be written as

$$t_F \approx \frac{1}{\hat{W}}\ln[1 + W_F](\dot{\varepsilon}_S)^{-1} = M_2(\dot{\varepsilon}_S)^{-1} \tag{10}$$

which is a Monkman-Grant relation of Eq (1a) with $M = \frac{1}{\hat{W}}\ln[1 + W_F]$, $\rho = 1$ and the minimum creep rate $\dot{\varepsilon}_M$ replaced with the theoretical secondary creep rate $\dot{\varepsilon}_S$. The MG constant M_2 will only be a true constant if both $\hat{W}$ and W_F are independent of test conditions. But $\hat{W}$ is the reciprocal of θ_3 which is known to be weakly dependent on test conditions, whilst W_F depends on ε_F and θ_1 which are also weakly dependent on test conditions.

The role of primary creep in the determination of time to failure is limited to $\dot{\varepsilon}_S$, which in turn is determined by the rate of hardening relative to the rate of recovery. The larger is the rate of recovery relative to the rate of hardening, the higher will be the secondary creep rate and consequently the smaller will be the time taken to fail. Eq (10) also makes it clear that the Monkman-Grant constant M_2 depends on several factors. Tertiary creep determines the time to failure through the amount of damage accumulated during tertiary creep and the rate at which this damage accumulates. The version of the Monkman-Grant relation given by Eq (10) results from the assumed mechanism that the role of damage accumulation in creep is to accelerate the secondary creep rate $\dot{\varepsilon}_S$. From Eq (10) it follows that failure times will be larger for a given secondary creep rate (i.e. M_2 will be larger) the more ductile is the material, i.e. the greater is the amount of tertiary strain $\varepsilon_F - \varepsilon_p$ and damage W (in the form of voids, precipitate morphology, alteration in grain boundary cavitation and cracking etc) that the material can absorb before failing.

There are therefore some similarities between this 4-θ Monkman-Grant relation and those proposed by Dobes and Milicka [11] and Abe [14]. In all three versions the exponent on the minimum (or secondary) creep rate is 1. Dobes and Milicka divide failure time by rupture strain, whilst Abe divided it by the strain at the end of primary creep. The 4-θ Monkman-Grant relation can therefore be considered as a combination of these two as it divides the failure time by $\ln\left[1 + \frac{\varepsilon_F - \varepsilon_p}{\theta_3}\right]$, i.e. by the difference between the rupture strain and strain at the end of primary creep. It can also be considered as a generalisation of these two versions as it also divides failure time by the rate of damage accumulation $(1/\theta_3)$ within a log transformation.

The effect of a change in the rate of damage accumulation on M_2 is less clear because an increase in $\widehat{W}$ will increase W_F but decrease $1/\widehat{W}$. It can be shown that the derivative of M_2 with respect to $\widehat{W}$ is negative (see Appendix A), and so an increase in the rate of damage accumulation will decrease the failure time at a given secondary creep rate. This can be written as

$$M_2 = f(^{+}W_F, {}^{-}\widehat{W}) \tag{11}$$

where the + and – signs indicate whether M_2 is positively or negatively related to the shown variable. In summary, the 4-θ methodology suggests M_2 will be larger the more the material can tolerate significant creep strain or stress relaxation before damage (e.g. voids, microcracks) leads to failure. It also suggests that M_2 will be larger the slower this damage accumulates over time. So, whether M_2 is independent of test conditions, depends on whether this materials ability to tolerate damage (and that rate of its accumulation over time) is determined by the test condition. Past studies on Ti-45Al-2Mn-2Nb [26] and Waspaloy [27] have shown that W_F depends directly on stress and indirectly on temperature via the material's tensile strength. The results section will later look at this in more detail.

Measuring minimum creep rates

The actual or observed creep rate at a given test condition is measured from the experimental creep curve. If such a curve is made up of i = 1 to n strain-time pairings, then the first step is to create a smoothed series for the experimental rates of strain using

$$\dot{\varepsilon}_i = \left\{ \frac{9\sum_{i=-4}^{4} \varepsilon_i t_i - \sum_{i=-4}^{4} \varepsilon_i \sum_{i=-4}^{4} t_i}{9\sum_{i=-4}^{4} t_i^2 - \sum_{i=-4}^{4} (t_i)^2} \right\} \quad (12)$$

where the subscript on t and ε denotes to the i^{th} measurement made for time and strain, respectively. Thus, the creep rate at time t_i is found by collecting the pairing $t_i\varepsilon_i$, the four $t_i\varepsilon_i$ pairings immediately below $t_i\varepsilon_i$ and the four $t_i\varepsilon_i$ pairings immediately above $t_i\varepsilon_i$ and putting a least squares linear line fit through these 9 data points. $\dot{\varepsilon}_i$ is then the slope of this best fit line.

Figure 3 shows this smoothed experimental strain rates obtained at 500MPa and 873K. The observed minimum creep rate is not taken to be the smallest observed value, but the mean of the strain rates along the flat part of the strain rate curve. This observed minimum strain rate is what is usually shown in papers when studying the Monkman-Grant relation and is therefore represented by the symbol $\dot{\varepsilon}_M$ (although authors use variations of the smoothing technique given by Eq (12)). For this test condition, the observed minimum creep rate is estimated at 1.74–08 s^{-1}. Such an estimate has a strong subjective component, because it is down to the researcher to identify exactly when the flat part of the curve starts and ends (in Figure 3 the curve has been truncated before the failure strain to allow the flat part of the curve to be seen more clearly).

In contrast to this, the theoretical secondary rate $\dot{\varepsilon}_S$ cannot be directly measured from the actual experimental creep curve when there is damage accumulating. Instead, Eq (2d) must be fitted to this experimental curve, to obtain estimates for θ_1 to θ_4 – see Evans [28,29] for details on such appropriate estimation or curve fitting techniques. If such estimates for θ_1 to θ_4 are represented by $\tilde{\theta}_1$ to $\tilde{\theta}_4$, then $\dot{\varepsilon}_S$ can be calculated as

$$\dot{\varepsilon}_S = \frac{\hat{R}}{\hat{H}} = \tilde{\theta}_3\tilde{\theta}_4 \quad (13a)$$

The rate of damage accumulation can be measured as

$$\hat{W} = \frac{1}{\tilde{\theta}_3} \quad (13b)$$

and so

$$\frac{\hat{R}}{\hat{H}}\hat{W} = \tilde{\theta}_4 \quad (13c)$$

All the other internal rates can also be measured from the parameters of the fitted creep curve

$$\dot{\varepsilon}_o = \tilde{\theta}_1\tilde{\theta}_2 + \tilde{\theta}_3\tilde{\theta}_4; \hat{H} = \frac{\tilde{\theta}_2}{\dot{\varepsilon}_o}; \hat{R} = \frac{\tilde{\theta}_2\tilde{\theta}_3\tilde{\theta}_4}{\dot{\varepsilon}_o} \quad (13d)$$

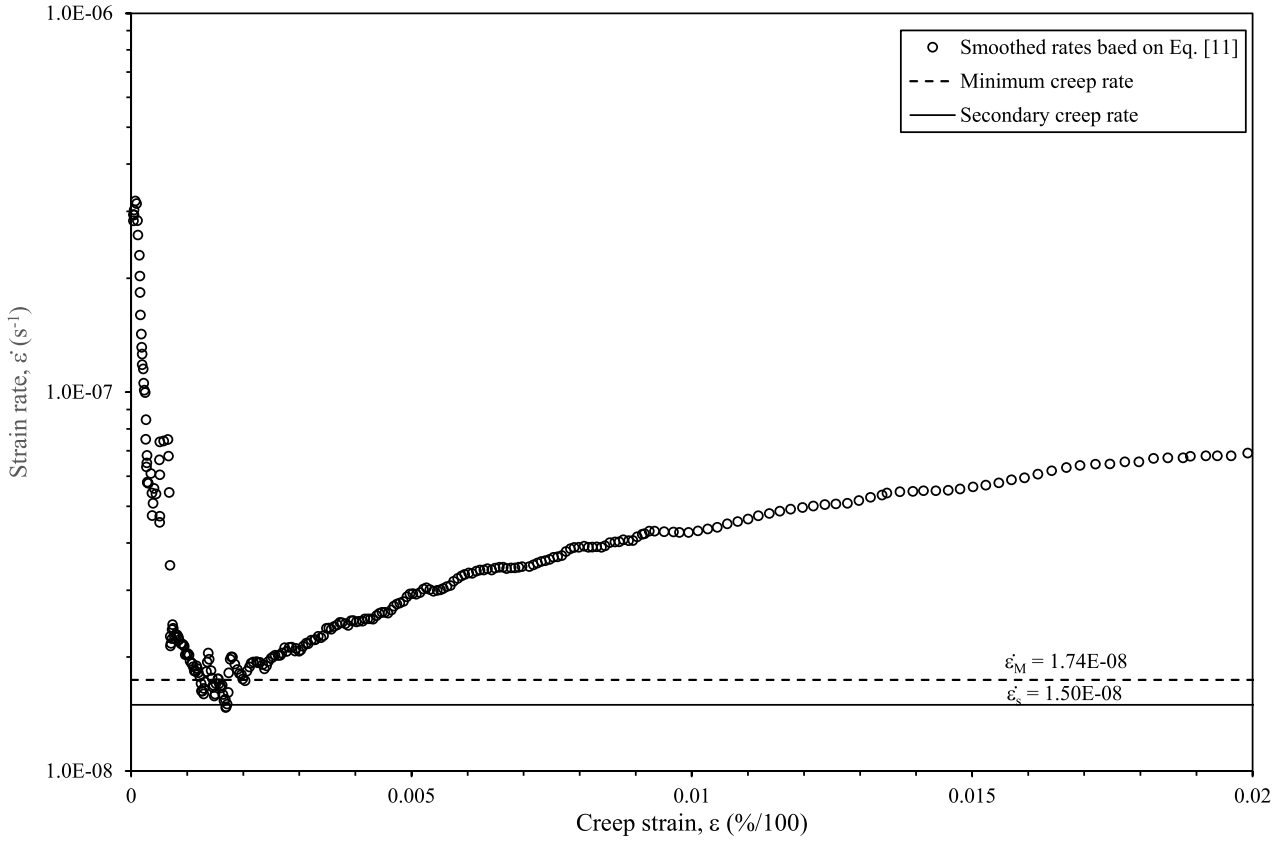

Figure 3. Smoothed experimental strain rates at 500MPa and 973K obtained using Eq (12), together with an estimate for the minimum creep rate and theoretical secondary rate.

At 500MPa and 973K the estimates for θ_3 and θ_4 are $\tilde{\theta}_3 = 0.004947$ and $\tilde{\theta}_4 = 3.02228\text{E–}06$ and so $\dot{\varepsilon}_S = \frac{\dot{R}}{H} = \tilde{\theta}_3\tilde{\theta}_4 = 1.50E-08$. There is no reason for $\dot{\varepsilon}_S$ to exactly equal $\dot{\varepsilon}_M$ as the former measure depends only on the rates of hardening and recover, whilst the latter measure obtained from the actual creep curve will contain some contributions from damage. If creep carried on without any damage the creep strain rates seen in Figure 3 would tend to the limit 1.50E − 08− which is slightly lower than that seen in the experimental curve where damage is contributing to the actual rates. They should, however, be similar in value at most test conditions (unless the damage rate is large early on).

Results

When applying Eq (1a) to all the experimental data outlined in the data section, $\rho = 0.778$ and $M = 1.2096$ for the best fit line seen in Figure 4. There is, however, a lot of variation around this relation, with it explaining only around 90% of the variation in failure times. There appears to be some points that appear to be well above the fitted line and some that are well below the line which may be an indication that the Monkman-Grant constant M is not truly constant.

The following subsections demonstrate that the data in Figure 4 fit into three distinctly different groupings depending on the value for M_2 and thus depending also on the tolerance to damage and the rate of damage accumulation. It is important to note that in the following analysis, three of the data points in Figure 4 had to be removed because for these points the tertiary creep strain was so small and the tertiary period so short lived that θ_1 and/or θ_2 could not be estimated. These three data points correspond to the test conditions 300 MPa at 973K and 1023K and 1023K at 250 MPa. For the rest of the data, Figure 5 plots the values for M_2 as calculated using Eq (10), against stress with the different symbols differentiating further with respect to temperature. Group 1a corresponds to test conditions producing M_2 values below 0.93%, whilst Group 1c corresponds to test conditions producing M_2 values above 4%. Group 1b corresponds to test conditions producing M_2 values in between these two limiting values.

Group 1c: relatively high values for M_2

Six data points make up this group and they correspond to all but one temperature (973K). They also tend to correspond to the largest stresses used at these temperatures. Thus, relatively high M_2 values are generated by high stresses irrespective of temperature. Figure 6 shows the creep curves corresponding to four of the six data points making up group 1c. The creep curves obtained at 1023K with 700 MPa and 873K with 1050 MPa have almost identical levels of strain and failure, but the specimen tested at 1023K, tolerated nearly twice the amount of damage before

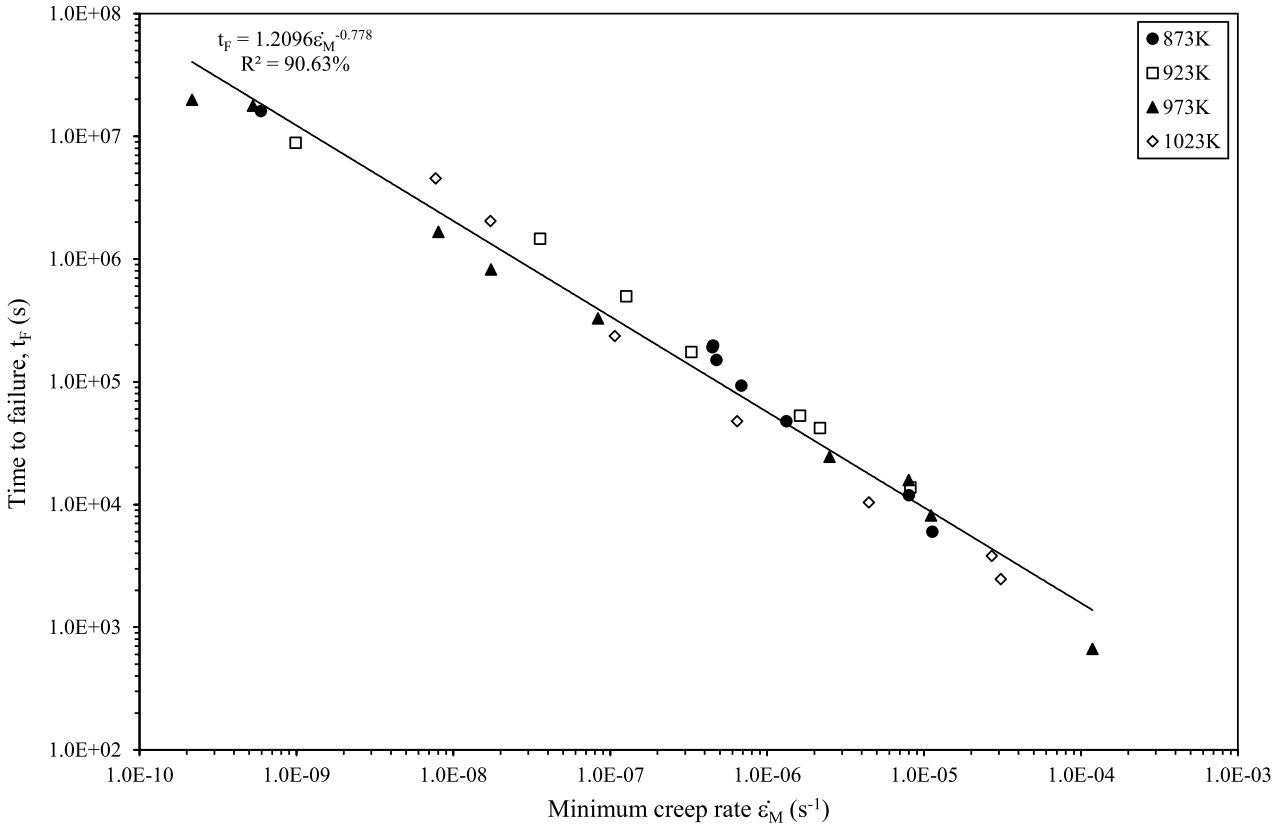

Figure 4. Variation in times to failure with the measured minimum creep rates, together with the least squares regression line.

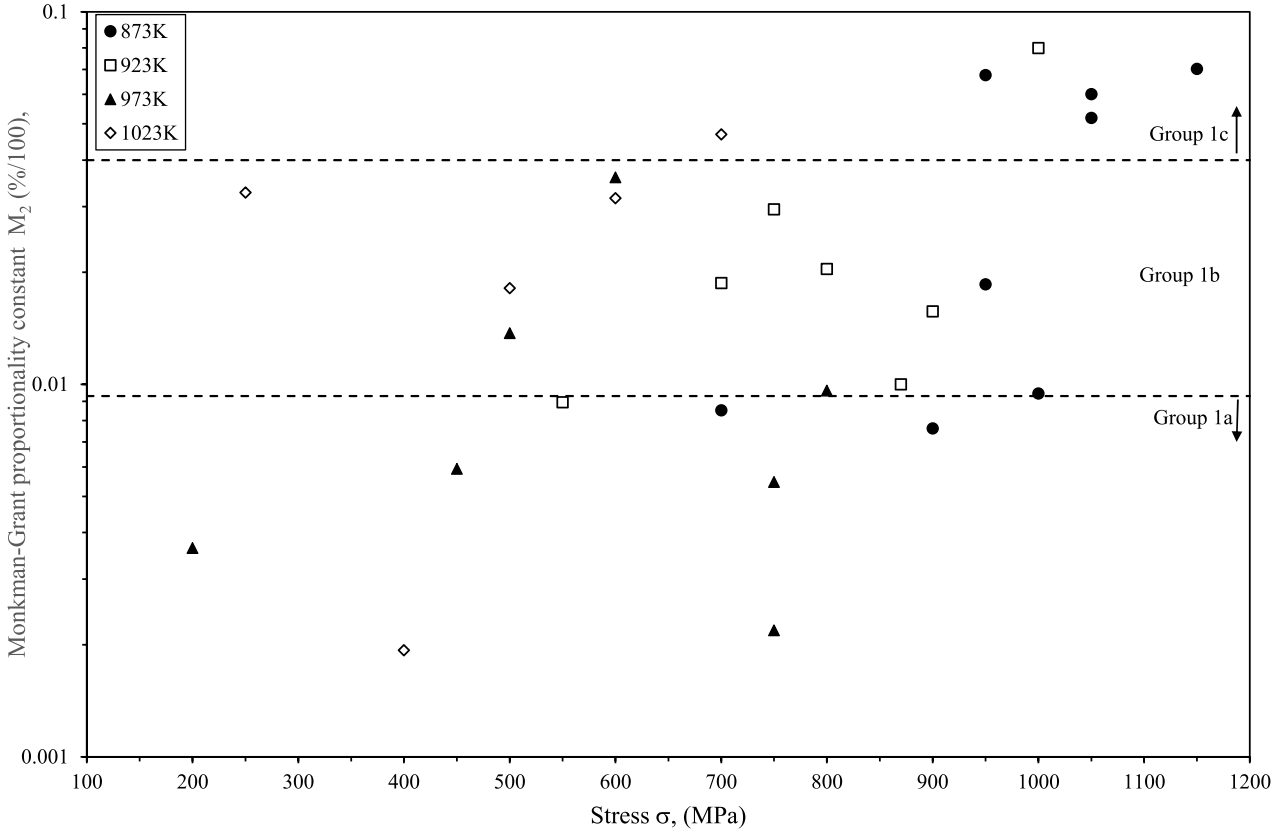

Figure 5. Variations in M_2, as calculated using Eq (10), with stress and temperature.

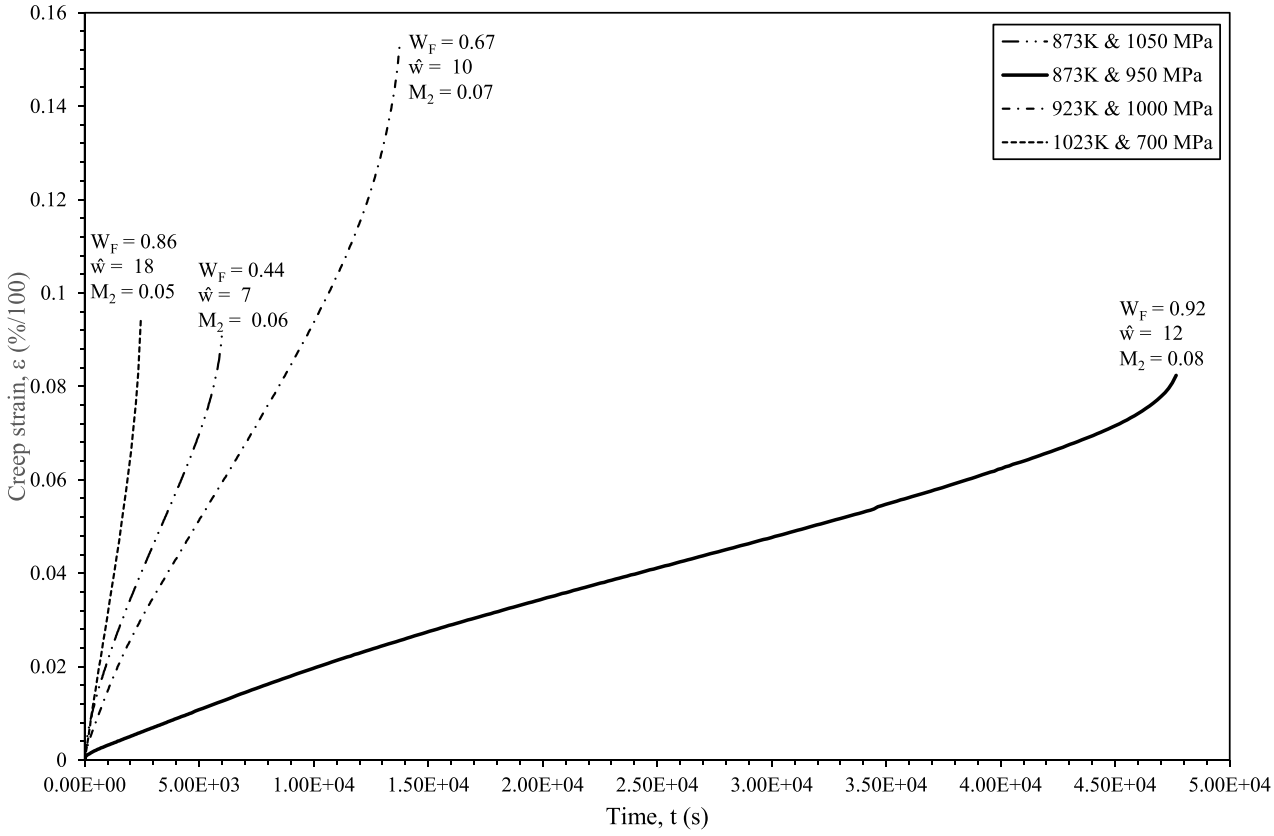

Figure 6. Some creep curves with M_2 values above 4% and so part of group 1c.

failing. Yet both specimens had very similar M_2 values, and this can be explained by the fact the specimen tested at 1023K accumulated damage at just over twice the rate of the specimen test at 873K. The creep curves obtained at 923K with 1000 MPa and 873K with 950 MPa have very similar rates of damage accumulation.

Yet both specimens had similar M_2 values, and this can be explained by the fact the specimen tested at 873K with 950 MPa, could tolerate more damage before failing. However, all the specimens in group 1c were characterised by low values for damage at failure – all below 1 in values – and low values for the rate of damage accumulation – all below 20. This can be appreciated from a glance at Figure 10 that displays the higher W_F values associated with the other two groupings. Within group 1c, a slightly higher value for W_F was compensated for by slightly lower values for the rate of damage accumulation resulting in M_2 always exceeding 4%.

Figure 7 plots the rates of creep corresponding to the creep curves in Figure 6. Another characteristic of the test results falling within group 1c is revealed in this Figure – namely most of the test time is taken up by declining creep rates or by primary creep followed by a much shorter period of secondary creep. Finally, there is a short period of accelerating creep or tertiary creep, which explains the low damage at failure values seen in test specimens within group 1c. The low rates of damage accumulation and small times spent in tertiary creep result in small amounts of damage accumulation by failure time.

Group 1b: relatively moderate M_2 values

The relatively moderate M_2 values associated with this group tend to occur at the moderate stress's for temperatures below 1023K but at low stresses at 1023K. The creep curves in Figure 8 obtained at 1023K and 250 MPa and 1023K and 500 MPa are in this group of moderate M_2 values (greater than 0.9% but less than 4%). The tolerance to damage at 250 MPa is roughly half that at 500 MPa, but because the rate at which this damage accumulates is approximately half that at 500 MPa, the failure time is substantially larger. The counterbalance between damage tolerance and rates of accumulation (one variable has a positive effect and the other a negative effect as explained in Eq (11)) result in these two specimens having the same value for M_2. When comparing these two creep curves to the creep curves seen in Figure 6, it becomes clear that the tolerance to damage is much higher, as is the rate of damage accumulation, both resulting in relatively moderate values for M_2.

Figure 9 shows the rates of creep associated with the creep curves in Figure 8. When comparing this to Figure 7 the time spent in tertiary creep is seen to be higher for specimens in group 1b compared to 1c. This fact combined with the realisation that the damage rate accumulation is lower for all curves in Figure 7 explains why the amount of damage accumulation before failure is higher in group 1b. This is more clearly seen in Figure 9, where all the tests in group 1c had lower amounts of damage at failure and lower rates of damage accumulation. Given that W_F has a positive effect on failure times and $\hat{W}$ a negative effect, the fact that specimens in group1b have a lower value for M_2 suggests the latter effect dominates the former.

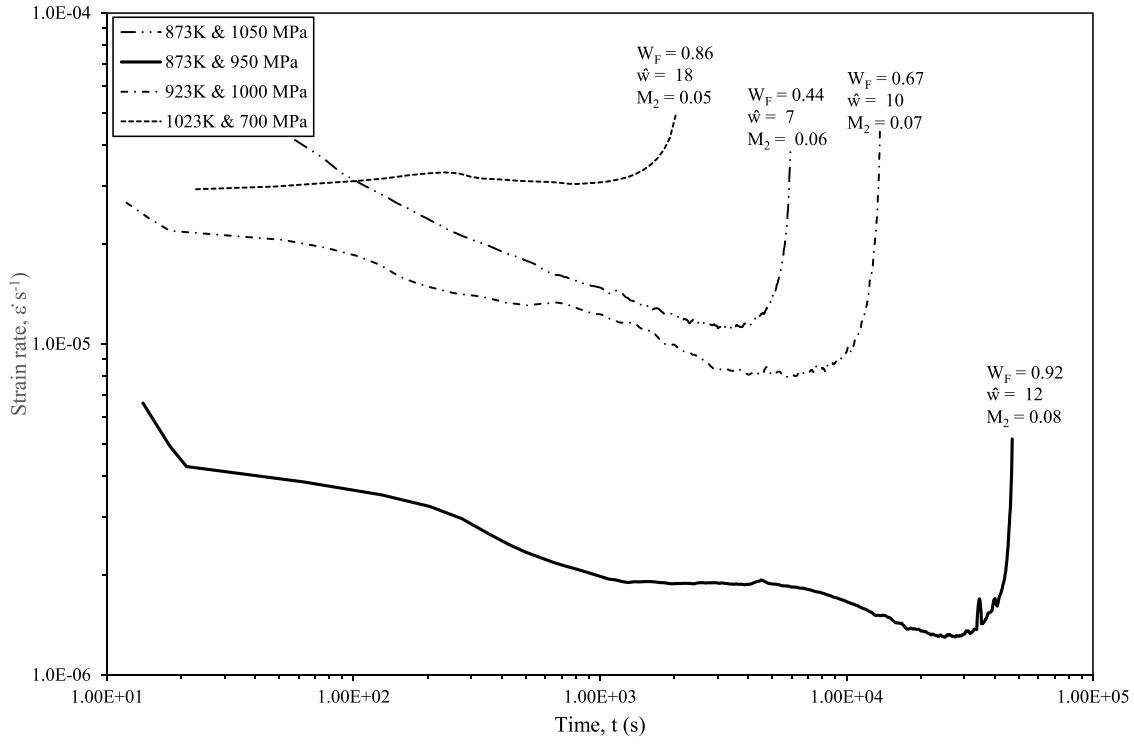

Figure 7. Rates of creep, obtained from Eq (12), that are associated with the creep curves displayed in Figure 6.

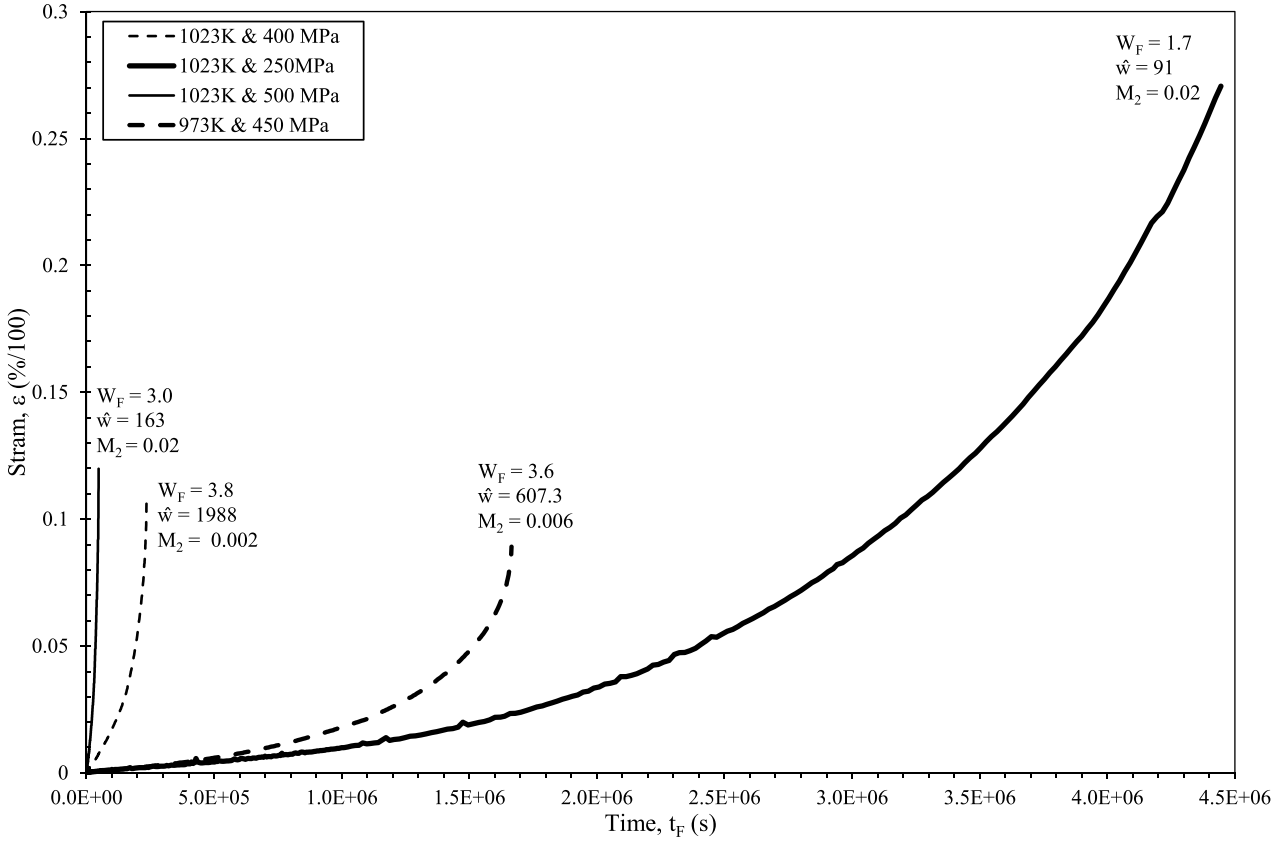

Figure 8. Two measured creep curves corresponding to groups 1a (obtained at 1023K with 400 MPa and at 973K with 450 MPa) and group 1b (obtained at 1023K with 400 MPa and at 1023K with 500 MPa).

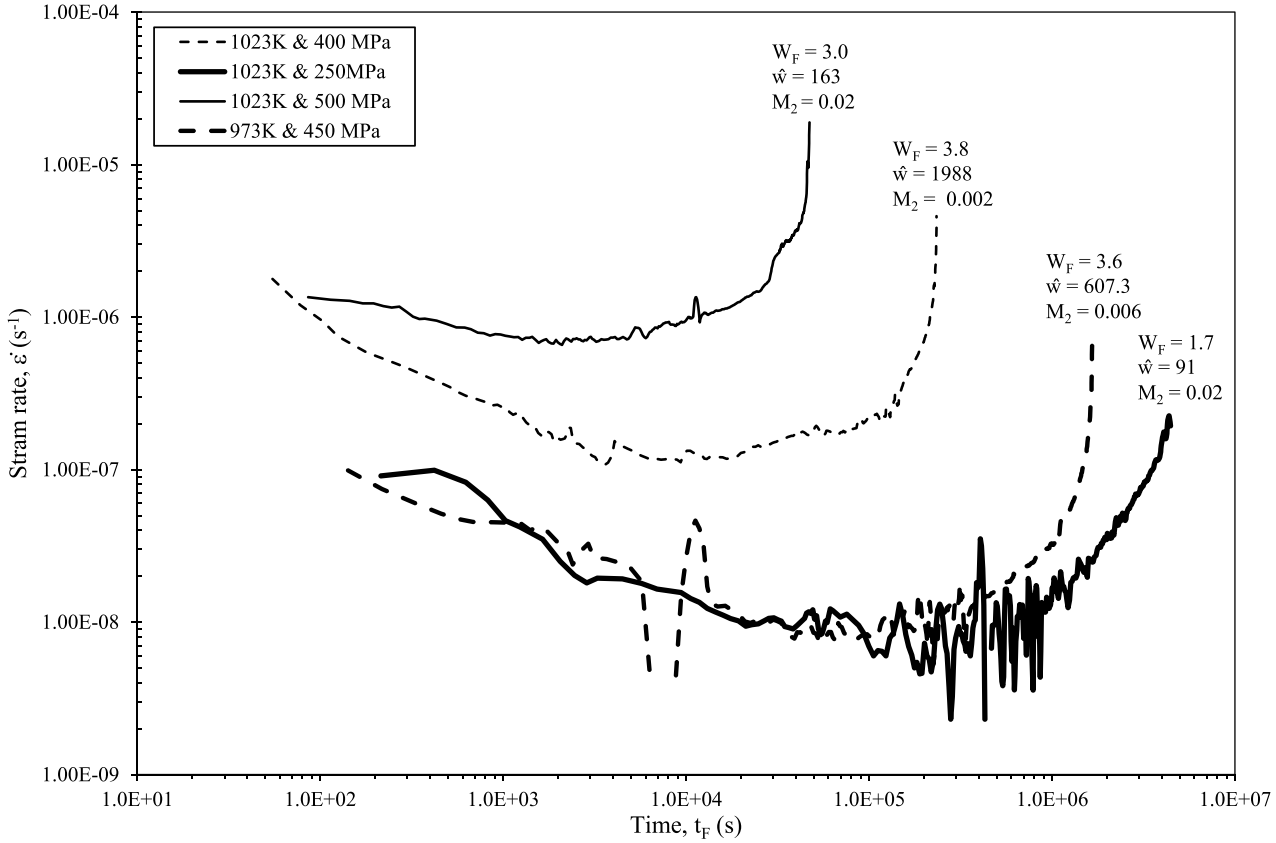

Figure 9. Rates of creep, obtained from Eq (12), that are associated with the creep curves displayed in Figure 8.

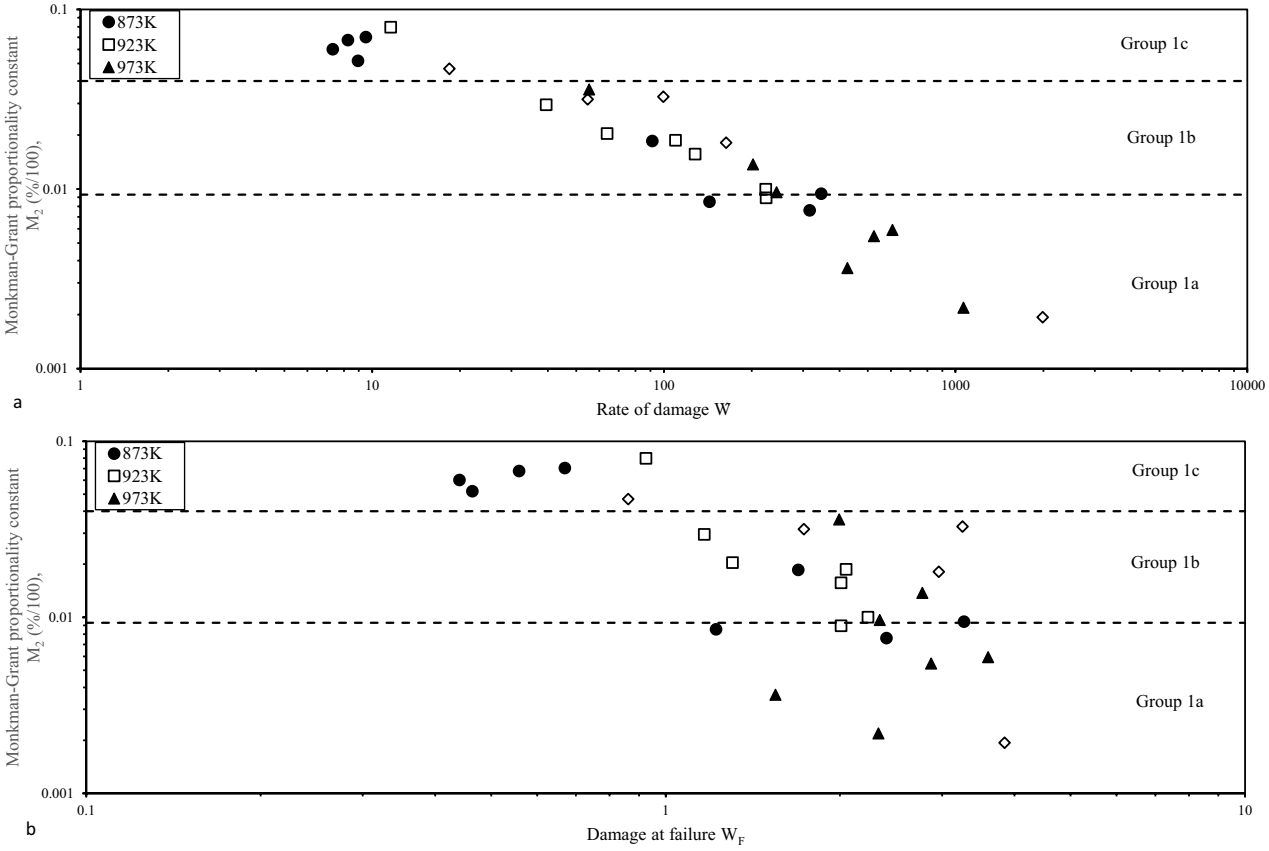

Figure 10. Variation in the Monkman-Grant constant M_2 values with a. rates of damage accumulation $\hat{W}$ and b. amounts of damage at failure W_F.

Group 1a: relatively low M_2 values

The relatively low M_2 values associated with this group tend to occur at the moderate to low stresses used at each temperature. The creep curves in Figure 8 obtained at 1023K and 400 MPa and 973K and 450 MPa are in this group of low M_2 value (less than 0.9%). The tolerance to damage at these two conditions are approximately the same, but because the rate at which this damage accumulates is appreciably lower at 973K with 450 MPa, the failure time is substantially smaller. The counterbalance between damage tolerance and rates of accumulation result in these two specimens having relatively low M_2 values.

The data in Figures 10 provides a further insight into the fundamental characteristics of the data points in groups 1a and 1b. Figure 10b plots values for M_2 against W_F and the data in groups 1a and 1b have broadly similar W_F values – in group 1a W_F is scattered around a mean value of 2.5, whilst in group 1b W_F is scattered around a mean value of 2.2. Yet the data in group 1b have higher M_2 values compared to those in group 1a. Figure 10a, which plots values for M_2 against $\hat{W}$, explains why. It is the result of the rate of damage accumulation being much lower in group 1b compared to group 1a – an average of 135 in group 1b compared to 662 in group 1a. And as Eq (10) reveals, lower values for $\hat{W}$ results in larger M_2 (and failure time) values. When comparing group 1c with group 1b specimens in group 1c have a much lower rate of damage accumulation (that results in a higher M_2 value) and whilst they have a lower damage at failure (that results in lower M_2 values) the former effect dominates and so results in specimens in group 1c having a higher value for M_2.

Thus, for tolerances to damage between 1 and 4, a low value for M_2 is caused by a relatively high rate of damage accumulation (between 100 sand 1100), whereas a rate of damage accumulation between 30 and 100 results in a moderate value for M_2. The defining characteristic for high M_2 values is very low rates of damage accumulation (20 or less). Even those specimens in this group also have low tolerance to damage this is more than offset by the lower rates of accumulation.

When studying Grade 92 steel, Maruyama et al. [13] identified four distinctly different regions when plotting failure times against stress (using iso-thermal lines). These regions had different creep mechanisms present and this led to distinctly different values for the Monkman-Grant exponent and Norton's n. That is, the groupings were defined by differences in ρ. This contrasts with the groupings 1a-c in this paper. These groupings are identified such that $\rho = 1$ in each of these three groupings (and so the Monkman-Grant

constant M_2 differed between the three groups). So, in this sense the groupings in this paper and that by Maruyama et al. are not directly comparable. In another sense, however, the groupings 1a-c are also defined in terms of creep mechanism (as is the case for 9Cr steel) in that in group 1a these mechanisms lead to low rates and amounts of damage accumulation, whilst in group 1c these mechanisms lead to high rates and amounts of damage accumulation. Whilst group 1b has similar amounts of damage at failure to group 1a, group 1b is characterised by creep mechanisms leading to intermediate rates of damage accumulation. Group 1a is therefore similar in nature to the low-stress region defined by Maruyama et al. that had the smallest rate of strain accumulation.

The flexibility of the theta methodology is that it allows for many different hardening, softening and damage mechanisms to play a role at any one time, but it does not need to specify them precisely to define overall hardening, softening and damage. Consequently, these three groupings are defined by the characteristics of such overall hardening, softening and damage. Thus, for example, group 1c is defined by high M_2 values caused by low amounts of damage at failure and by damage accumulating occurring at a slow rate. This does not preclude the possibility that the groupings are also defined by different creep mechanisms – it's just they are not used in the methodology to define these groups. That said, the data in Figure 5 at 873K may fall into groups 1b and 1c because of different creep mechanisms. In this figure, at this temperature, lower M_2 values are observed at approximately around 950 MPa, which is very close to the reported 0.2% proof stress for this material at this temperature [22].

This ties in with the work of Williams et al. [29] who reported that at 873 K, Waspaloy shows a mechanism change around the yield stress, which is ~ 920 MPa for typical test heats. Below ~ 900 MPa (≈below yield at 873 K), creep damage is dominated by diffusion-assisted processes: dislocation climb and grain-boundary activity, leading to intergranular cavitation/voiding. Above ~ 900 MPa, deformation is controlled by higher dislocation densities with forest-hardening and γ′ cutting, producing more trans granular/dislocation-controlled damage. When combined with the theta analysis this suggests that the low amounts of damage accumulated by failure for specimens in group 1c is trans granular in nature, whilst the higher accumulations of damage for specimens in group 1b takes the form of inter-granular voids. Attaching specific types of damage to the damage quantities in each group as identified using the theta methodology would form an interesting area of future research but is beyond the scope of this paper.

Failure times

Figure 11 shows the estimates made for the parameters of the Monkman-Grant relation of Eq (10) within each of the groupings identified above. The Monkman-Grant constant M_2 increases from 0.29% in group 1a to 2.48% in group 1b and to 4.33% in group 1c. These values correspond well with the average values for M_2

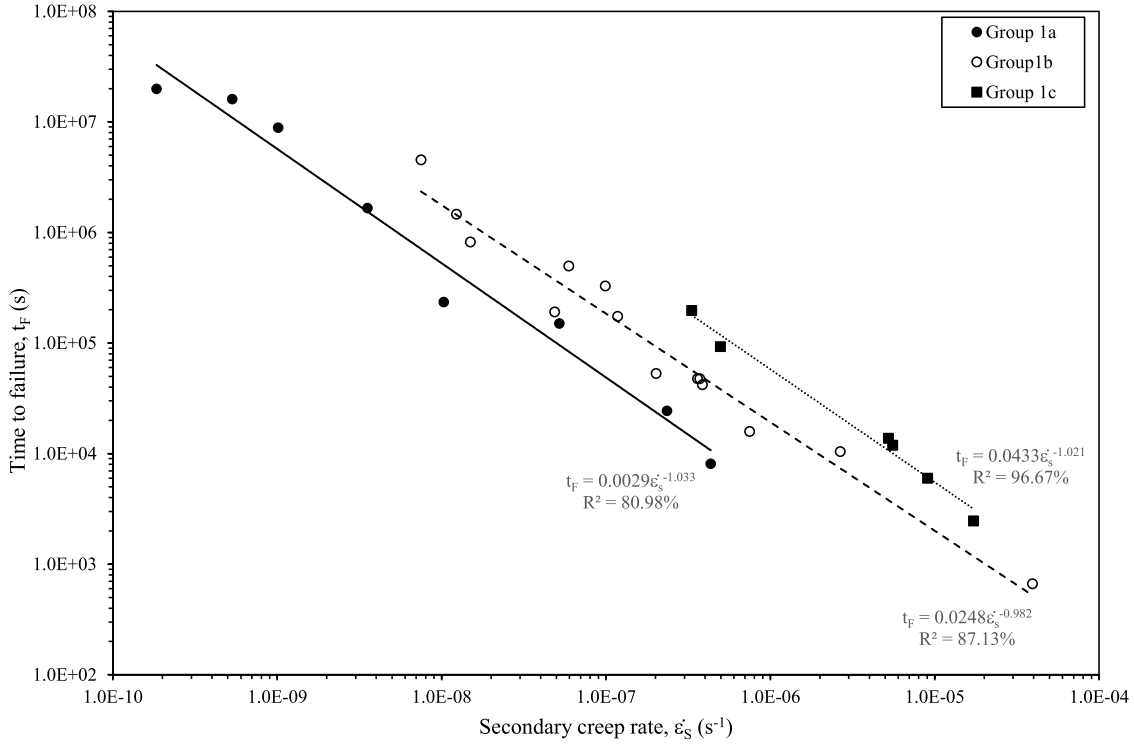

Figure 11. Variations in time to failure with the secondary creep rate, together with the estimated Monkman-Grant relation for each group of data.

in each group as shown in the second column of Table 3. The statistical significance of the seen difference in these sample mean M_2 values can be tested using the following t-value

$$\text{t} - \text{value} = \frac{\left(\bar{M}_{2,1} - \bar{M}_{2,2}\right) - \left(\mu_1 - \mu_2\right)}{\sqrt{\frac{s_1^2}{n_1} + \frac{s_2^2}{n_2}}} \qquad (14a)$$

where μ_1 is the population (true) mean value for M_2 for damage conditions that place results within one of the three groups seen in Figure 9 and μ_2 is the population (true) mean value for M_2 for damage conditions that place results within another of the three groups seen in Figure 9. This test statistic allows for unequal variances between the groupings. $\bar{M}_{2,1}$ and $\bar{M}_{2,2}$ are the corresponding estimated means from samples of size n_1 and n_2, with $s^2{}_1$ and s_{22} being the sample variances. Under the null hypothesis that the true mean values for M_2 between two groupings are the same ($Ho : \mu_1 - \mu_2 = 0$), this t-value follows (approximately) a student t distribution with degrees of freedom (d.f.) estimated as

$$\text{d.f.} = \frac{\left(\frac{s_1^2}{n_1} + \frac{s_2^2}{n_2}\right)^2}{\frac{1}{n_1 - 1}\left(\frac{s_1^2}{n_1}\right)^2 + \frac{1}{n_2 - 1}\left(\frac{s_2^2}{n_2}\right)^2} \qquad (14b)$$

These t-values for mean comparisons are shown in the one but last column of Table 3. Thus, the t-value of −11.22 tests the null hypothesis that the difference between the true mean values for M_2 in group 1a and group 1c are the same. Based on the t-value, the probability that this null hypothesis is true is 0.01%. So, at the 1% significance level, the mean value for M_2 in these two groups are different, i.e. the negative value for the sample mean difference of (0.0055–0.0628) has not occurred by chance. Table 3 reveals that the three mean values are all statistically significantly different from each other at the 1% significance, so that the best fit lines in Figure 11 differ from each other in a statistically significant way.

This difference takes the form of a parallel shift as damage characteristics change. That is, $\rho = 1$ in all three groupings. Even in group 1a where ρ is estimated at 1.033, this is not significantly different from 1 – the p-value for the null hypothesis that the true value for ρ is 1 is 63%. There is therefore a very high probability that the true value for ρ is 1 (it would come out as 1 if there were many more data points available). The p-values for testing $\rho = 1$ in the other two groups are 74% for group 1b and 76% for group 1c. Thus, once account is taken for different amounts and rates of damage accumulation, the true value for ρ is 1, irrespective of these differences in damage characteristics. $\rho = 1$ is as predicted by the 4-θ methodology.

To further confirm the validity of the 4-θ Monkman-Grant relation, the data points in Figure 11 are replotted in Figure 12 according to Eq (10). The gradient of −0.997 of the regression line in Figure 12 corresponds to the exponent on $\dot{\varepsilon}_s$ in Eq (10) and so is as predicted by the 4-θ methodology. The proportional coefficient of 1.041 is close to the value of 1 that is predicted by the 4-θ methodology. Indeed, the p-value for testing that the population value for this proportional coefficient equals 1 comes out at 72% and so this hypothesis cannot be rejected – even as the 10% significance level. Unlike in Figures 4 and 11, all the data points are closely packed around one regression line, contrary to their larger deviations in Figure 4 around a single regression line and around multiple lines in Figure 11.

For the relation in Figure 12 to be of any use in reducing the length of the development cycle for new materials two things need to be considered, First, the extent to which W_F and $\hat{W}$ can be accurately extrapolated from accelerated test condition needs to be assessed. This is really beyond the scope of this paper, but this would form an interesting and necessary area for future research. Second, the secondary creep rate must be measurable in relatively short-time periods. This question can be briefly addressed here using a plot of $\dot{\varepsilon}_S$ against $\dot{\varepsilon}_M$ as in Figure 13. Within each grouping these is a very strong and clear relationship between these two measures. Typically, $\dot{\varepsilon}_M$ can be measured by running tests for around 30% of creep life. One approach to measuring $\dot{\varepsilon}_S$ within the same time span is therefore to first find $\dot{\varepsilon}_M$ and insert it into

Table 3. Mean values for M_2 in each grouping, together with tests for the statistical significance of differences between these means.

	Monkman-Grant constant M_2				
Group	Mean	Standard Deviation	d.f.	t-value	p-value
Group 1a	0.0055	0.00275	17	−5.85[a]	0.0025
Group 1b	0.0208	0.00908	5	−11.22[b]	0.010
Group 1c	0.0628	0.01227	7	−7.54[c]	0.0013

d.f. is the degrees of freedom as calculated using Eq (14). p-value is the probability (in %) that there is no difference between the population mean values in the groupings listed below:

a. This is the student t statistic for testing for a statistically significant difference between the population mean value for M_2 in group 1a and group 1b.

b. This is the student t statistic for testing for a statistically significant difference between the population mean value for M_2 in group 1a and group 1c.

c. This is the student t statistic for testing for a statistically significant difference between the population mean value for M_2 in group 1b and group 1c.

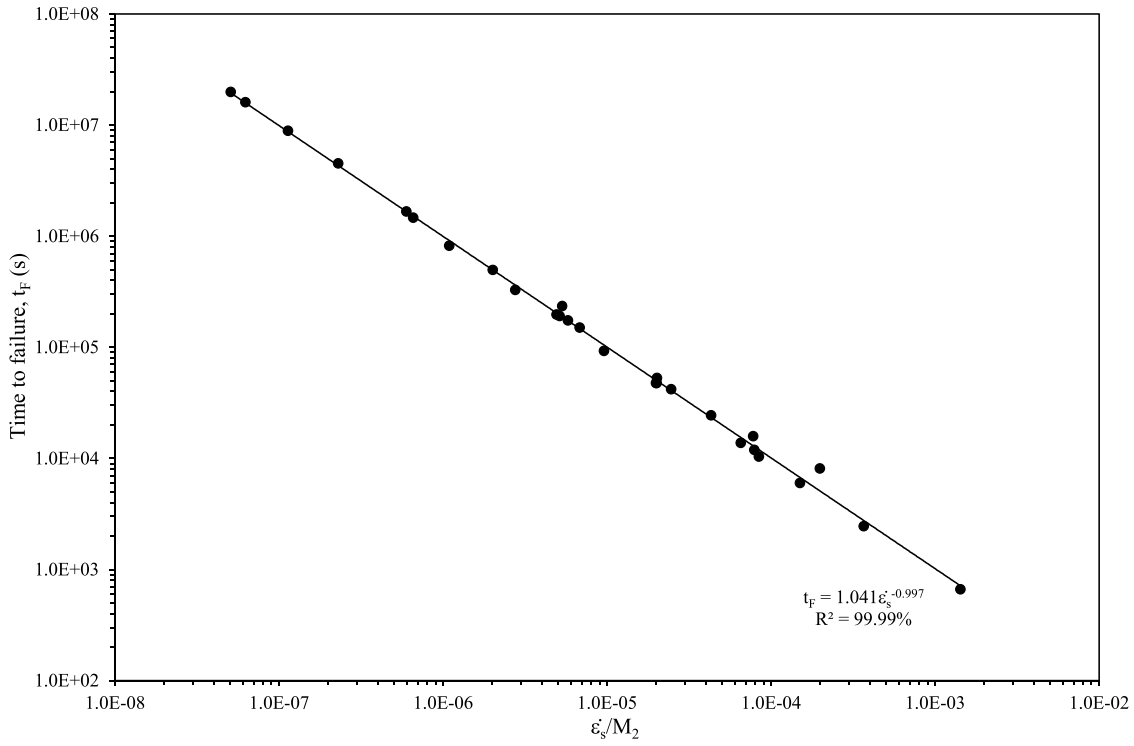

Figure 12. The modified 4-θ Monkman-Grant relation.

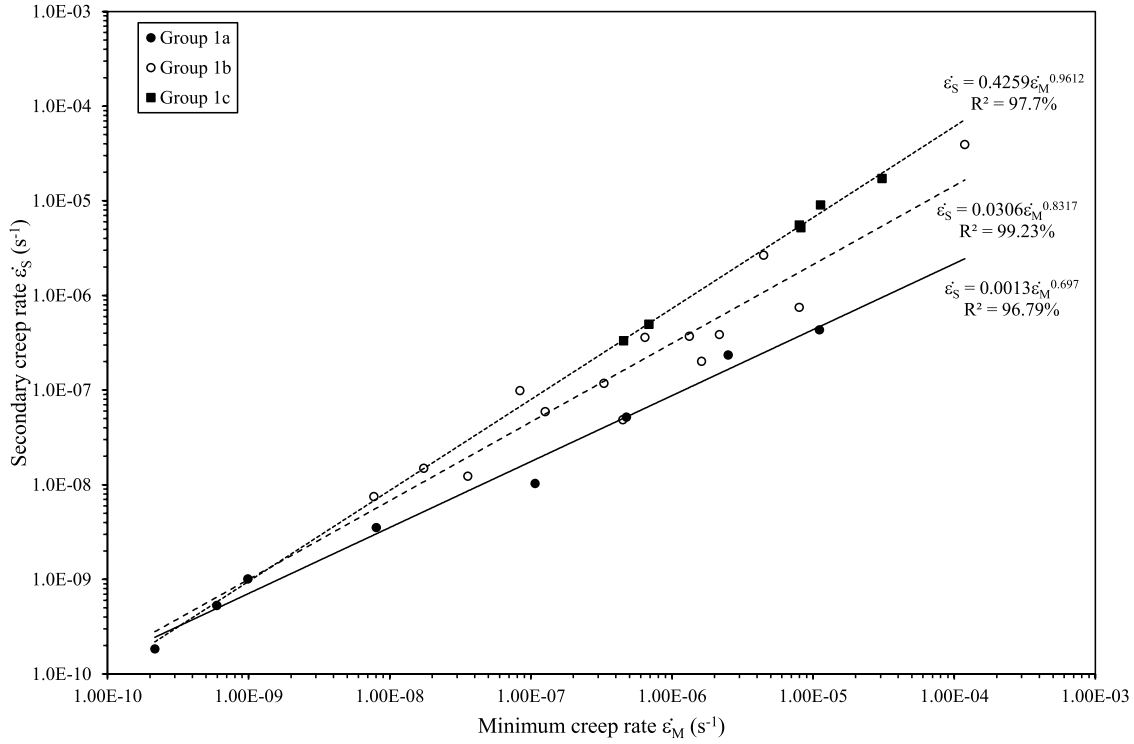

Figure 13. The variation in $\dot{\varepsilon}_S$ with $\dot{\varepsilon}_M$.

the equations present in Figure 13 to find the corresponding value for $\dot{\varepsilon}_S$. As the R^2 vales in this figure are between 97% and 99%, this approach should determine $\dot{\varepsilon}_S$ with a high degree of accuracy. The only remaining question would then be which of these groupings is most relevant for the typical operating conditions experienced by Waspaloy? This could form another area for future research but once known, the M_2 value to use in Figure 12 are found by averaging the M_2 values in Figure 5 for that grouping, i.e. use the value shown in column 2 of Table 3.

Conclusions

The Monkman-Grant relation offers the possibility of reducing the cost and length of the development cycle for new materials operating at high temperatures by using minimum creep rates that can be obtained relatively quickly even at low stresses. This paper used the 4-θ methodology to i. identify and explain the form of this relation in terms of creep mechanisms such as hardening, recover and damage and ii. to discover whether this form was compatible with long-term creep life assessment. The 4-θ methodology suggests that the traditionally measured minimum creep rate should be replaced by the theoretical minimum creep rate measured as $\theta_3\theta_4$. It also predicts that the exponent on this secondary creep rate will equal −1. This methodology also predicted that the Monkman-Grant proportionality constant (M_2) was positively related to the amount of strain during tertiary creep, positively related to the total amount of damage accumulated during this stage but negatively related to the rate at which damage accumulates. The methodology also suggested that the role played by primary creep in identifying the form of the Monkman-Grant relation was restricted to the determination of the theoretical secondary creep rate.

These predictions were confirmed by the data obtained on Waspaloy steel. Without considering any of these causal variables, the exponent on the minimum creep rate was considerably different from the 4-θ prediction that it should equal −1 (−0.778). However, it was also found that the values for the Monkman-Grant proportionality constant (M_2) fell into three well-defined groupings depending on the amount of accumulated damage and the rate at which it occurred. Two of the groupings had similar amounts of damage at failure, but different rates of damage accumulation that split the data into relatively low and moderate M_2 values. It then turned out that within each such grouping, the exponent on the secondary creep rate equalled −1. The other grouping had rates of damage accumulation and damage at failure below those seen in groups 1a,1b. An interesting area for future research therefore is to study this possibility for reducing the development cycle for new materials in more detail by assessing the extent to which W_F and $\hat{W}$ can be accurately extrapolated from accelerated test conditions. If they can, then the value for M_2 can be found for typical operating conditions for this material. Eq (10) would then allow a failure time prediction to be made as well. Other areas of future research include identifying the relevant group for the typical operating conditions for Waspaloy and approaches for quantifying $\dot{\varepsilon}_S$ in shorter time spans than that required for finding $\dot{\varepsilon}_M$ – by, for example, extrapolating the theta creep curve equation that excludes damage accumulation.

Disclosure statement

There are no patents or copyrights that are relevant to the work in the manuscript.

There is nothing else of merit to declare.

Funding

The author received no financial support for the research, authorship, and/or publication of this article. There are no financial interest or relationship — within the last 3 years — related to the subject matter but not directly to this manuscript.

References

[1] Yang M, Wang Q, Song XL, et al. On the prediction of long-term creep strength of creep resistant steels. Int J Mater Res. 2016;107(2):133–138. doi: 10.3139/146.111322

[2] Wilshire B, Battenbough AJ. Creep and creep fracture of polycrystalline copper. Mater Sci Eng, A. 2007;443(1–2):156–166. doi: 10.1016/j.msea.2006.08.094

[3] Wilshire B and Scharning PJ. Prediction of long term creep data for forged 1Cr–1Mo–0·25V steel. Mater Sci Technol. 2008;24(1):1–9. doi: 10.1179/174328407X245779

[4] Wilshire B and Whittaker M. Long term creep life prediction for grade 22 (2.25Cr-1Mo) steels. Mater Sci Technol. 2001;27(3):642–647. doi: 10.1179/026708310X520529

[5] Wilshire B, Scharning PJ. A new methodology for analysis of creep and creep fracture data for 9–12% chromium steels. Int Mater Rev. 2008;53(2):91–104. doi: 10.1179/174328008X254349

[6] Whittaker MT, Evans M, Wilshire B. Long-term creep data prediction for type 316H stainless steel. Mater Sci Eng A. 2012;552:145–150. doi: 10.1016/j.msea.2012.05.023

[7] Monkman FC, Grant NJ. An empirical relationship between fracture life and minimum creep rate in creep rupture tests. Proc Of Am Soc For Test Mater. 1956;56:593–605.

[8] Machlin ES. Creep rupture by vacancy condensation. Transaction Of Am Inst For Met. 1956;8(2):106. doi: 10.1007/BF03377651

[9] Abe F. Creep behaviour, deformation mechanisms, and creep life of Mod.9Cr-1Mo steel. Metall Mater Trans A. 2015;46(12):5610–5625. doi: 10.1007/s11661-015-3144-5

[10] Choudhary BK. Tertiary creep behaviour of 9Cr-1Mo steel. Mater Sci Eng: A. 2013;585:585 1–9. doi: 10.1016/j.msea.2013.07.026

[11] Dobes F, Milicka K. The relation between minimum creep rate and time to fracture. Metal Sci. 1976;10(11):382–384. doi: 10.1080/03063453.1976.11683560

[12] Sklenicka V, Kucharova K, Kral P, et al. Applicability of empirical formulas and fractography for assessment of creep life and creep fracture modes of tempered martensitic 9%Cr steel. Kovove Mater. 2017;55(2):69–80. doi: 10.4149/km_2017_2_69

[13] Maruyama K, Sekido N, Yoshimi K. Changes in Monkman-Grant relation among four creep regions of modified 9Cr-1Mo steel. Mater Sci Eng: A. 2019;749:223–234. doi: 10.1016/j.msea.2019.02.003

[14] Abe F. Modified version of Monkman-Grant equation for Gr.91 by incorporating "strain to minimum creep rate" parameter. Int J Press Vessels And piping. 2022;200:104815. doi: 10.1016/j.ijpvp.2022.104815
[15] Evans RW, Wilshire B. Creep of metals and alloys. London, Appendix: Institute of Metals; 1985.
[16] Evans RW. A constitutive model for the high-temperature creep of particle-hardened alloys based on the Θ projection method. R Soc Proc: Math, Phys And Eng Sci. 2000;456(1996):835–868. doi: 10.1098/rspa.2000.0539
[17] Wilshire B, Scharning PJ. Theoretical and practical approaches to creep of Waspaloy. Mater Sci & Technol. 2009;25(2):242–248. doi: 10.1179/174328408X361508
[18] Mrozowski N, Hénaff G, Hamon F, et al. Aging of γ′ precipitates at 750 °C in the nickel-based superalloy AD730TM: a thermally or thermo-mechanically controlled process? Metals. 2020;10(4):426. doi: 10.3390/met10040426
[19] Chamanfar A, Jahazi M, Gholipour J. Modeling grain size and strain rate in linear friction welded Waspaloy. Metall Mater Trans A. 2013;44(9):4230–4238. doi: 10.1007/s11661-013-1767-y
[20] Neri MA, Martinez –Villafane A, Carreno C, et al. Cobarrubias-Alvarado metallurgical characterization of Waspaloy presenting variations in chemical composition, grain size and hardness. The Miner, Met And Mater Soc. 2012.
[21] Chaudhari R, Ayesta I, Doshi M, et al. Implementation of passing vehicle search algorithm for optimization of WEDM process of nickel-based superalloy waspaloy. Nanomater (Basel). 2022 Dec 9;12(24):4394. doi: 10.3390/nano12244394
[22] Whittaker M, Harrison W, Deen C, et al. Creep deformation by dislocation movement in Waspaloy. Materials. 2017;10(1):61. doi: 10.3390/ma10010061
[23] Chen K, Dong J, Yao Z. Creep failure and damage mechanism of Inconel 718 alloy at 800–900 °C. Met Mater Int. 2021;27(5):970–984. doi: 10.1007/s12540-019-00447-4
[24] Yao Z, Zhang M, Dong J. Stress rupture fracture model and microstructure evolution for Waspaloy. Metall Mater Trans A. 2013;44(7):3084–3098. doi: 10.1007/s11661-013-1660-8
[25] Wen J-F, Tu S-T, Xuan F-Z, et al. Effects of stress level and stress state on creep ductility: evaluation of different models. J Mater Sci & Technol. 2016;32(8):695–704. doi: 10.1016/j.jmst.2016.02.014
[26] Harrison W. Creep modelling of Ti6246 and Waspaloy using Abaqus [PhD thesis]. (UK): University of Wales Swansea; 2007.
[27] Harrison W, Whittaker M, Gray V. Advanced methods for creep in engineering design. In: Tanski T, Sroka M Zielinski A, editors. Creep. 2018. IntechOpen. doi: 10.5772/intechopen.68393
[28] Evans RW. Statistical scatter and variability of creep property estimates in θ projection method. Mater Sci Technol. 1989;5(7):699–707. doi: 10.1179/mst.1989.5.7.699
[29] Williams T, Evans M, Harrison W. An investigation into the correlation of small punch and uniaxial creep data for Waspaloy. Metall Mater Trans A. 2021;52(8):3460–3474. doi: 10.1007/s11661-021-06318-1

Appendix A.

Here a short confirmation that the derivative of M_2 with respect to $\hat{W}$ is negative. From Eq (10)

$$M_2 = \frac{1}{\hat{W}}\ln[1 + W_F] = \frac{1}{\hat{W}}\ln\left[1 + \hat{W}\mathrm{x}\right] \tag{A1}$$

where $\mathrm{X} = \left(\varepsilon_{\mathrm{F}} - \varepsilon_{\mathrm{p}}\right)$. Using the quotient rule for differentiation

$$\frac{\mathrm{dM}_2}{\mathrm{d}\hat{\mathrm{W}}} = \frac{\frac{\widehat{\mathrm{Wx}}}{\widehat{1+\mathrm{Wx}}} - \ln\left[1 + \widehat{\mathrm{Wx}}\right]}{\hat{\mathrm{W}}^2} \tag{A2}$$

Next, define $\mathrm{u} = \hat{\mathrm{W}}\mathrm{x}$ and $\mathrm{h(u)}$ as

$$h(u) \;=\; \hat{\mathrm{W}}^2\,\frac{dm}{dw} \;=\; \frac{u}{1+u} - \ln\,[1+u] \tag{A3}$$

It needs to be shown that $\mathrm{h(u)} < 0$ for all $\mathrm{u} \geq 1$, $\mathrm{u} \neq 0$ because $\ln(1+\mathrm{u})$ is only defined for $\ln(1+\mathrm{u}) > 0$. The derivative of $\mathrm{h(u)}$ with respect to u is

$$\frac{dh(u)}{\mathrm{du}} = \frac{-u}{(1+u)^2} \tag{A4}$$

So, if $\mathrm{u} > 0$ then $\frac{dh(u)}{\mathrm{du}} < 0$ and so this derivative function is decreasing in u. If $\mathrm{u} < 0$ then $\frac{dh(u)}{\mathrm{du}} > 0$ and so this derivative function is increasing in u. Further, $h(0) = 0$, $h(u) < 0$ when $\mathrm{u} > 0$ and $h(u) < 0$ when $\mathrm{u} < 0$. Thereforeh

$$h(u) = \frac{u}{1+\mathrm{u}} - \ln[1+\mathrm{u}] \;< 0 \text{ for u } 0 >\tag{A5}$$

and thus

$$\frac{\mathrm{dM}_2}{d\hat{W}} = \frac{f(u)}{\hat{W}^2} = \frac{f\left(\hat{W}x\right)}{\hat{W}^2} < 0 \tag{A6}$$